Chapter 8
Deterministic and Statistical Size Effect in Plain Concrete

Abstract. The numerical FE investigations of a deterministic and stochastic size effect in concrete beams of a similar geometry under three point bending were performed within an elasto-plasticity with a non-local softening. The FE analyses were carried out with four different sizes of notched and unnotched beams. Deterministic calculations were performed with a uniform distribution of the tensile strength. In turn, in stochastic calculations, the tensile strength took the form of random correlated spatial fields described by a truncated Gaussian distribution. In order to reduce the number of stochastic realizations without losing the calculation accuracy, Latin hypercube sampling was applied. The numerical outcomes were compared with the size effect law by Bažant and by Carpinteri.

A size effect phenomenon (nominal strength varies with the size of structure) is an inherent property of the behaviour of many engineering materials. In the case of concrete materials, both the nominal strength and material brittleness (ratio between the energy consumed during the loading process after and before the stress-strain peak) always decrease with increasing element size under tension (Bažant 1984, Carpinteri 1989, Bažant and Planas 1998). Thus, concrete becomes perfectly brittle on a sufficiently large scale. The results from laboratory tests which are scaled versions of the actual structures cannot be directly transferred to them. The physical understanding of size effects is of major importance for civil engineers who try to extrapolate experimental outcomes at laboratory scale to results which can be used in big scale situations. Since large structures are beyond the range of testing in laboratories, their design has to rely on a realistic extrapolation of testing results with smaller element sizes.

Two size effects are of a major importance in quasi-brittle and brittle materials: deterministic and statistical one (the remaining size effects are: boundary layer effect, diffusion phenomena, hydration heat or phenomena associated with chemical reactions and fractal nature of crack surfaces) (Bažant and Planas 1998). Currently there exist two different theories of size effect in quasi-brittle structures:

J. Tejchman, J. Bobiński: Continuous & Discontinuous Modelling of Fracture, SSGG, pp. 297–341.
springerlink.com

the energetic-statistical theory (Bažant and Planas 1998, Bažant 2004) and fractal theory (Carpinteri et al. 1994, 1995).

According to Bažant and Planas (1998) and Bažant (2004) the deterministic size effect is caused by the formation of a region of intense strain localization with a certain volume (micro-crack region - called also fracture process zone FPZ) which precedes macro-cracks and cannot be appropriately scaled in laboratory tests. Strain localization volume is not negligible to the cross-section dimensions and is large enough to cause significant stress redistribution in the structure and associated energy release. The specimen strength increases with increasing ratio l_c/D (l_c – characteristic length of the micro-structure influencing both the size and spacing of localized zones, D – characteristic structure size). In turn, a statistical (stochastic) effect is caused by the spatial variability/randomness of the local material strength. The first statistical theory was introduced by Weibull (1951) (called also the weakest link theory) which postulates that a structure is as strong as its weakest component. The structure fails when its strength is exceeded in the weakest spot, since stress redistribution is not considered. The Weibull's size effect model is a power law and is of particular important for large structures that fail as soon as a macroscopic fracture initiates in one small material element. It is not however able to account for a spatial correlation between local material properties, does not include any characteristic length of micro-structure (i.e. it ignores a deterministic size effect) and it underestimates the experimental size effect. Combining the energetic theory with the Weibull statistical theory led to a general energetic-statistical theory (Bažant and Planas 1998). The deterministic size effect was obtained for not too large structures and the Weibull statistical size effect was obtained as the asymptotic limit for very large structures. In turn, according to Carpinteri et al. (1994, 1995, 2007), the size effect is caused by the multi-fractality of a fracture surface only which increases with a spreading disorder of the material in large structures (stress redistribution and energy release during strain localization and cracking are not considered).

Two size effects laws proposed by Bažant (Bažant and Planas 1998, Bažant 2004) (called Size Effect Laws SEL) for geometrically similar structures allow to take into account a size difference by determining the tensile strength of structures without notches and pre-existing large cracks (the so-called type 1 size effect law) and of notched structures or structures with pre-existing cracks (the so-called type 2 size effect law) (Fig. 8.1). In the first type structures, the maximum load is reached as soon as a macroscopic crack initiates from the fully formed localized region of non-negligible size developed at a smooth surface. In the second type structures, cracks grow in a stable manner prior to the maximum load. Only the first type of structures is significantly affected by material randomness causing a pronounced statistical size effect. The material strength is bound for small sizes by a plasticity limit whereas for large sizes the material follows linear elastic fracture mechanics.

The following analytical formulae for a deterministic size effect predicted by asymptotic matching were proposed by Bažant (Bažant and Planas 1998)

$$\sigma_N(D) = f_r^{\infty}\left(1+\frac{rD_b}{D}\right)^{\frac{1}{r}} \text{ (type 1 size effect law SEL)} \tag{8.1}$$

and

$$\sigma_N(D) = \frac{Bf_t}{\sqrt{1+\frac{D}{D_o}}} \text{ (type 2 size effect law SEL),} \tag{8.2}$$

where σ_N is the nominal strength, D is the characteristic structure size, f_r^{∞}, D_b and r denote the positive constant representing unknown empirical parameters to be determined; f_r^{∞} represents the solution of the elastic-brittle strength reached as the nominal strength for large structures, r controls the curvature and shape of the law and D_b is the deterministic characteristic length having the meaning of the thickness of the cracked layer (if D_b=0, the behaviour is elastic-brittle, Eq. 8.1). In turn, in Eq. 8.2, f_t denotes the tensile strength, B is the dimensionless geometry-dependent parameter (depending on the geometry of the structure and crack) and D_o denotes the size-dependent parameter called transitional size (both unknown parameters to be determined).

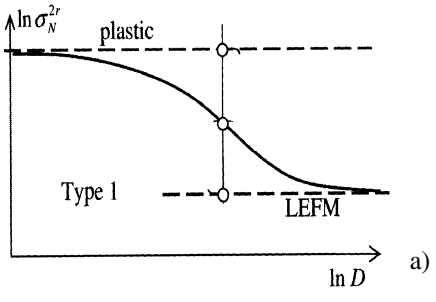

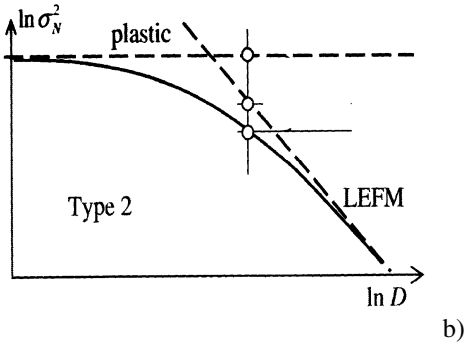

Fig. 8.1 Size effect models SEL by Bažant (2004) in logarithmic scale with σ_N - nominal strength, D – element size: a) type 1 (structures without notches and pre-existing large cracks), b) type 2 (notched structures) (material strength is bound for small sizes by plasticity limit whereas for large sizes, the material follows Linear Elastic Fracture Mechanics LEFM)

Another approach to the size effect was proposed by Carpinteri et al. (1994, 1995, 2007) (called Multi-Fractal Scaling Law MFSL) (Fig. 8.2). In this fractal approach, the nominal strength σ_N under tension decreases in a hyperbolic form with increasing characteristic structure size D

$$\sigma_N(D) = \sqrt{A_1 + (A_2 / D)}, \tag{8.3}$$

where A_1 and A_2 are the empirical constants. The approach does not distinguish between a deterministic or statistical size effect. The MFSL behaviour in the bilogarithmic plane $\ln\sigma_N$ versus $\ln D$ is non-linear and shows two asymptotes with slope -1/2 for small structures and slope zero for the largest ones, respectively. It predicts a transition from a disordered regime at the smallest scales to an ordered regime at the largest scales. According to Bažant and Yavari (2005, 2007c), the cause of a size effect is certainly energetic-statistical not fractal and the multi-fractal scaling law is a purely empirical formula and good enough only for the type 1 size effect (at crack initiation) and only for sizes not so large that the Weibull statistical size effect would intervene (MFSL does not capture a transition to the Weibull size effect for very large sizes). The disadvantage of both size effect laws is that they do not explicitly present the empirical constants to calculate the size effect in advance. In addition, a transition between two size effect types by Bažant remains still to be challenge.

The fits of the size effect law by Bažant (2004) and the multi-fractal scaling law by Carpintieri et al. (1994) to experimental data for concrete elements (van Vliet 2000) and reinforced concrete beams failing by shear (Bažant and Yavari 2007 c) show that both laws are only similar for experiments at laboratory scale but can significantly differ when the structure is very small or very large (Fig. 8.3) that can have serious consequences in the second case.

In spite of many experiments exhibiting the noticed size effect in concrete and reinforced concrete elements under different loading types (Walraven and Leihwalter 1994, Wittmann et al.1990, Elices et al. 1992, Bažant and Chen 1997,

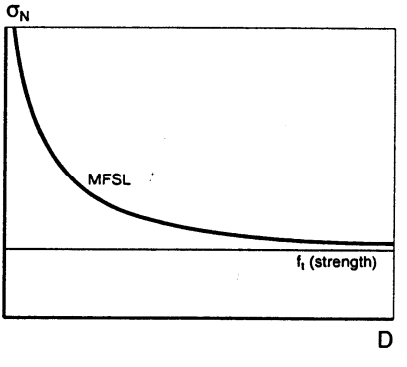

Fig. 8.2 Size effect by Carpintieri et al (1994): nominal strength σ_N versus specimen size D

Bažant and Planas 1998, Koide et al. 1998, van Vliet 2000, Chen et al. 2001, Le Bellego et al. 2003, van Mier and van Vliet 2003, Bažant 2004, Bažant and Yavari 2005, Vorechovsky 2007, Yu 2007), the scientifically (physically) based size effect is not taken into account in a practical design of engineering structures, that may contribute to their failure (Bažant and Planas 1998, Yu 2007). Instead, a purely empirical approach is sometimes considered in building codes which is doomed to yield an incorrect formula since physical foundations are lacking.

The goal of the numerical simulations is to investigate a deterministic and statistical size effect mainly in flexural resistance of notched and un-notched beam elements of a similar geometry under quasi-static three-point bending by considering the influence of strain localization. A finite element method with an elasto-plastic constitutive model using a Rankine'a criterion with non-local softening (Eqs. 3.32, 3.93 and 3.97) was used. Two-dimensional calculations were performed with four different concrete beam sizes of a similar geometry. Deterministic calculations were performed assuming constant values of tensile strength. In turn, statistical analyses were carried out with spatially correlated homogeneous distributions of tensile strength which were assumed to be random. Truncated Gaussian random tensile strength fields were generated using a conditional rejection method (Walukiewicz et al. 1997) for correlated random fields. The approximated results were obtained using a Latin hypercube sampling method (McKay et al. 1979, Bažant and Lin 1985, Florian 1992, Huntington and Lyrintzis 1998) belonging to a group of variance reduced Monte Carlo methods (Hurtado and Barbat 1998). This approach enables one a significant reduction of the sample number without losing the accuracy of calculations. The numerical results of load-displacements diagrams with notched beams were compared with corresponding laboratory tests performed by Le Bellego et al. (2003). The effect of the correlation length was also investigated. The FE results were compared with the size effect law SEL by Bažant and MFSL by Carpinteri.

The combined statistical and deterministic size effects were simulated by Carmeliet and Hens (1994), Frantziskonis (1998), Gutierrez and de Borst (1998), Gutierrez (2006), Vorechovsky (2007), Bažant et al. (2007a, 2007b), Yang and Xu (2008) and Bobiński et al. (2009). The most comprehensive combined calculations were performed by Vorechovsky (2007) for unnotched concrete specimens under uniaxial tension with a micro-plane material model and crack band model using Latin hypercube sampling. A squared exponential autocorrelation function with a correlation length of 80 mm was used. His results showed that the strength of many specimens, which parameters were obtained from random sampling, could be larger than a deterministic one in small specimens in contrast to large specimens which rather obeyed the weakest link model. The difference between a deterministic material strength and a mean statistical strength grew with increasing size. The structural strength exhibited a gradual transition from Gaussian distribution to Weibull distribution at increasing size. As the ratio of autocorrelation length and specimen size decreased, the ratio of spatial fluctuation of random field realizations grew. In the work by Yang and Xu (2008), a

heterogeneous cohesive crack model to predict macroscopic strength of materials based on meso-scale random fields of fracture properties was proposed. A concrete notched beam subjected to mixed-mode fracture was modeled. Effects of various important parameters on the crack paths, peak loads, macroscopic ductility and overall reliability (including the variance of random fields, the correlation length, and the shear fracture resistance) were investigated and discussed.

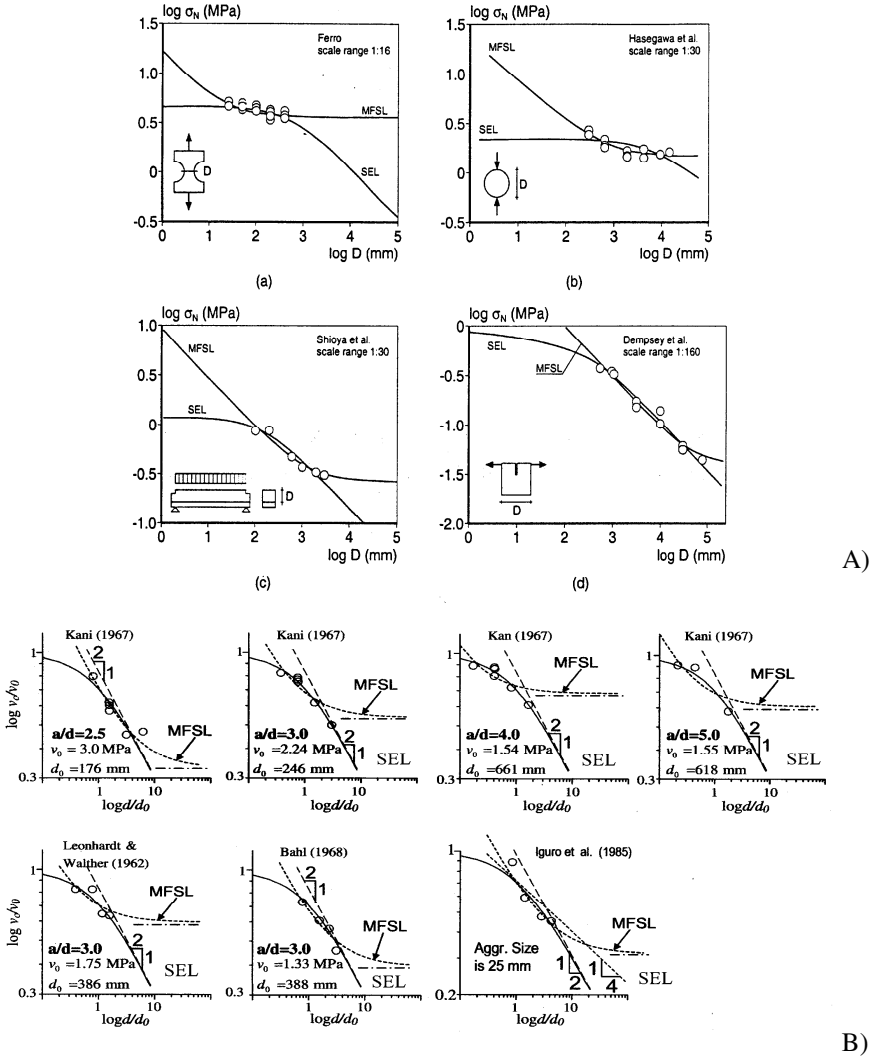

Fig. 8.3 Fits of the Size Effect Law by Bažant (2003) (SEL) and the Multi Fractal Scaling Law by Carpintier et al (1994) (MFSL) to experimental data: A) for concrete elements (van Vliet 2000) and B) for reinforced concrete beams failing by shear (Bažant and Yavari 2007c)

Our calculations with beams follow the research presented by Vorechovsky (2004, 2007) by using an alternative stochastic approach. In contrast to his simulations: a) free-supported concrete beams under bending were analyzed, b) a more sophisticated regularization technique was used in the softening regime, namely non-local theory, which ensured entirely mesh–independent results with respect to load-displacement diagrams and widths of localized zones (in contrast to the crack band model which provides only mesh-independent load-displacement diagrams), c) an original method of the random field generation with a different homogeneous correlation function was used.

In addition, a deterministic effect was examined in concrete during uniaxial compression using a Drucker-Prager's criterion with non-local softening (Eqs. 3.27-3.30, 3.93 and 3.97).

8.1 Notched Beams

Deterministic and statistical calculations

The two-dimensional FE-calculations (Bobiński et al. 2009) of free supported notched beams with free ends under bending (assuming constant values of tensile strength f_t) were performed with 4 different beam sizes of a similar geometry $h \times L_t$: 8×32 cm^2 (called small-size beam), 16×64 cm^2 (called medium-size beam), 32×128 cm^2 (called large-size beam) and 192×768 cm^2 (called very large-size beam) (h – beam height, L_t – total beam length). The span length L was equal to $3h$ for all beams (Fig. 8.4). The size of the first 3 beams was similar as in corresponding experiments carried out by Le Bellego et al. (2003). The quadrilateral elements divided into triangular elements were used to avoid volumetric locking. 7628 triangular (small-size beam), 14476 (medium-size beam), 28092 (large size beam) and 104310 (large-size beam) triangular elements were used, respectively. The mesh was particularly very fine in the region of a notch (Fig. 8.5) to properly capture strain localization in concrete (where the finite element size was equal to $1/3 \times l_c$, l_c=5 mm). The ratio between the width of this fine region and beam length was always the same.

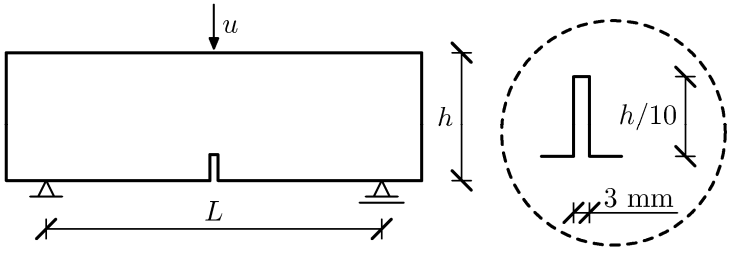

Fig. 8.4 Notched concrete beams used for calculations (L=3×h) (Bobiński et al. 2009)

To describe the behaviour of concrete under tension during three-point bending, a Rankine criterion was used with a yield function with isotropic softening (Eq. 3.32). To model the concrete softening under tension, the exponential curve by Hordijk (1991) with the tensile strength of the concrete of f_t=3.6 MPa was assumed (κ_u=0.005 b_1=3.0, b_2=6.93) (Eq. 3.55). The modulus of elasticity was assumed to be E=38.5 GPa and the Poisson ratio was υ=0.24 (Le Bellego et al. 2003). The calculations were performed under plane strain conditions (the differences between the results obtained within Rankine plasticity under plane stress and plane strain conditions are insignificant). A large-displacement analysis available in the ABAQUS finite element code (1998) was used (although the influence of such analysis was negligible). In this method, the current configuration of the body was taken into account. The Cauchy stress was taken as the stress measure. The conjugate strain rate was the rate of deformation. The rotation of the stress and strain tensor was calculated with the Hughes-Winget method (1980). The non-local averaging was performed in the current configuration.

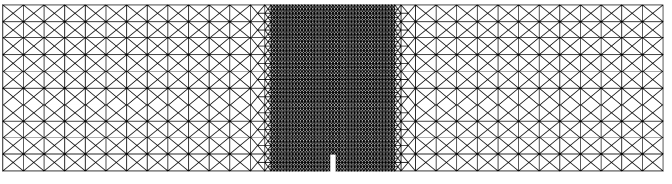

Fig. 8.5 FE mesh in the case of a medium-size beam (Bobiński et al. 2009)

A quasi-static deformation of a small, medium and large beam was imposed through a constant vertical displacement increment $\Delta \boldsymbol{u}$ prescribed at the upper mid-point of the beam top. To capture a snap-back behaviour in a very large size beam, the so-called arc-length technique was used. The actual load vector $\boldsymbol{P}$ was defined as $\lambda \boldsymbol{P}_{\max}$ where λ – multiplier and $\boldsymbol{P}_{\max}$ – maximum constant load vector. In general, the determination of the length of the arc the $\boldsymbol{P}$–$\boldsymbol{u}$ space ($\boldsymbol{u}$ – displacement vector) involves the displacements of all nodes (as e.g. the Riks method available in ABAQUS Standard 1998). However, for problems involving strain localization, it is more suitable to use an indirect displacement control method, where only selected nodal displacements are considered to formulate an additional condition in the $\boldsymbol{P}$–$\boldsymbol{u}$ space. The horizontal distance between two nodes lying on the opposite sides of the notch was chosen as a control variable *CMOD* (crack mouth open displacement). The indirect displacement algorithm was implemented with the aid of two identical and independent FE-meshes and some additional node elements to exchange the information about the displacements between these meshes.

The Monte Carlo method was used in statistical calculations. Application of the method in stochastic problems of mechanics requires the following steps: simulation of random variables or fields describing the problem under

consideration (variability of material parameters, initial imperfections in structure geometrics and others), solution of the problem for each simulated realization, creation of a set of results and its statistical description. Contrary to stochastic finite element codes, the Monte Carlo method does not impose any restriction to the solved random problems. Its only limitation is the time of calculations. For example, to reproduce exactly the input random data of initial geometric imperfection of a shell structure problem, at least 2000 random samples should be used (Bielewicz and Górski 2002). Any nonlinear calculations for such number of initial data are, however, impossible due to excessive computation times. To determine a minimal, but sufficient number of samples (which allows one to estimate the results with a specified accuracy), a convergence analysis of the outcomes was proposed (Górski 2006). It was estimated that in case of various engineering problems only ca. 50 realizations had to be considered. For example in the shell structure limit load analysis (Górski 2006), the change of the error of limit load mean values between 50 and 150 samples equaled 2% and the standard deviations error was 12%. A further decrease of sample numbers can be obtained using Monte Carlo variance reduction methods.

In the papers by Tejchman and Górski (2007, 2008), two methods: a stratified and a Latin sampling method were considered. It should be pointed out that these methods were not used for the generation of two-dimensional random fields as, for example, in the paper by Vorechovsky (2007), but for their classification. For that reason, the single realization was generated according to the initial data, i.e. the theoretical mean value and the covariance matrix was exactly reproduced. The statistical calculations according to the proposed version of the Latin sampling method were performed in two steps (Tejchman and Górski 2007, 2008). First, an initial set of random samples was generated in the same way as in the case of a direct Monte Carlo method. Next, the generated samples were classified and arranged in increasing order according to the chosen parameters (i.e. their mean values and the gap between the lowest and the highest values of the fields). From each subset defined in this way, only one sample was chosen for the analysis. The selection was performed in agreement with the theoretical background of the Latin sampling method. The numerical calculations were performed only for these samples. It was proved that using the Latin sampling variance reduction method the results can be properly estimated by several realizations only (e.g. 12-15) (Tejchman and Górski 2007, 2008).

To generate the random field, the original conditional-rejection method described by Walukiewicz et al. (1997), Bielewicz and Górski (2002), Górski (2006), Tejchman and Górski (2007), and Tejchman and Górski (2008) was used. The method makes it possible to simulate any homogeneous or non-homogeneous truncated Gaussian random field described on regular or irregular spatial meshes. An important role in the calculations was played by the propagation base scheme covering sequentially the mesh points and the random field envelope which allowed one to fulfill the geometric and boundary conditions of the structure of the model. Random fields of practically unlimited sizes could be generated.

Various properties of concrete may be considered as randomly distributed. In the present work, only fluctuations of its tensile strength were taken into account. Two parameters described the random field should be chosen, i.e. the distribution of the random variable in a single point of the field and a function defining the correlation between these points. The distribution of a single random variable took the form of a truncated Gaussian function with the mean concrete tensile strength of $\bar{f}_t = 3.6$ MPa. Additionally, it was assumed that the concrete tensile strength values changed between f_t=1.6 MPa and f_t=5.6 MPa ($f_t = 3.6 \pm 2.0$ MPa). To fulfil this condition, the standard deviation $s_{f_t} = 0.424$ MPa was used in the calculations. The coefficient of variations describing the field scattering was $\mathrm{cov} = s_{f_t} / \bar{f}_t = 0.118$ ($\bar{f}_t$=3.6 MPa - the mean tensile strength). Since $5s_{f_t} = 5 \times 0.424 = 2.12$ MPa, the cut of variables did not change the theoretical Gauss distribution distinctly (Fig. 8.6). The Irvin's characteristic length $(EG_f)/f_t^2$ (G_f - tensile fracture energy) which controls the length of the fracture process zone (Bažant and Planas 1998) varied between 0.100 m and 0.351 m.

Randomness of tensile strength f_t has to be described by a correlation function. For lack of the appropriate data, the correlation function is usually chosen arbitrarily. It is evident that the fluctuation of any material parameters should be described by a homogeneous function, which confirms that the correlation between random material variables vanishes when the random point distance increases. Any non-homogeneous correlation function, for example Wiener or Brown, defines strong correlation between every point of the field, and such a definition of material parameters is unrealistic. The simplest choice is a standard first order correlation function $K(x_1, x_2) = e^{-\lambda_{x_1} \Delta x_1} e^{-\lambda_{x_2} \Delta x_2}$. Here, the following (more general) second order and homogeneous correlation function was adopted (Bielewicz and Gorski 2002)

$$K(\Delta x_1, \Delta x_2) = s_{f_t}^2 \times e^{-\lambda_{x_1} \Delta x_1} (1 + \lambda_{x_1} \Delta x_1) e^{-\lambda_{x_2} \Delta x_2} (1 + \lambda_{x_2} \Delta x_2), \tag{8.4}$$

where Δx_1 and Δx_2 is are the distances between two field points along the horizontal axis x_1 and vertical axis x_2, λ_{x1} and λ_{x2} are the decay coefficients (damping parameters) characterizing a spatial variability of the specimen properties (i.e. describe the correlation between the random field points). The second order homogeneous function (Eq. 8.4) was proved to be very useful in engineering calculations (Knabe et al. 1998).

In finite element methods, continuous correlation function (Eq. 8.4) has to be represented by the appropriate covariance matrix. For this purpose, the procedure of local averages of the random fields proposed by Vanmarcke (1983) was

adopted. After an appropriate integration of the function (Eq. 8.4), the following expressions describing the variances D_w and covariances K_w were obtained (Knabe et al. 1998)

$$D_w(\Delta x_1,\Delta x_2)=\frac{2}{\lambda_{x_1}\Delta x_1}s_{f_t}^2\left[2+e^{-\lambda_{x_1}\Delta x_1}-\frac{3}{\lambda_{x_1}\Delta x_1}\left(1-e^{-\lambda_{x_1}\Delta x_1}\right)\right]\times$$
$$\times\frac{2}{\lambda_{x_2}\Delta x_2}s_{f_t}^2\left[2+e^{-\lambda_{x_2}\Delta x_2}-\frac{3}{\lambda_{x_2}\Delta x_2}\left(1-e^{-\lambda_{x_2}\Delta x_2}\right)\right], \quad (8.5)$$

$$K_w(\Delta x_1,\Delta x_2)=\frac{e^{\lambda_{x_1}\Delta x_1}}{\left(\lambda_{x_1}\Delta x_1\right)^2}s_{f_t}^2\left\{\left[\cos\left(\lambda_{x_1}\Delta x_1\right)-\sin\left(\lambda_{x_1}\Delta x_1\right)\right]+2\lambda_{x_1}\Delta x_1-1\right\}\times$$
$$\times\frac{e^{\lambda_{x_2}\Delta x_2}}{\left(\lambda_{x_2}\Delta x_2\right)^2}s_{f_t}^2\left\{\left[\cos\left(\lambda_{x_2}\Delta x_2\right)-\sin\left(\lambda_{x_2}\Delta x_2\right)\right]+2\lambda_{x_2}\Delta x_2-1\right\}. \quad (8.6)$$

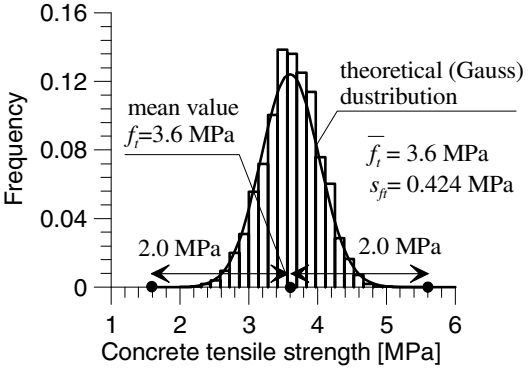

Fig. 8.6 Distribution of the concrete strength values for a single point of the mesh (Bobiński et al. 2009)

We took mainly into account a strong correlation of the tensile strength f_t in a horizontal direction λ_{x1}=1 1/m and a weaker in a vertical direction λ_{x2}=3 1/m in Eq. 8.4 (due to the way of specimen's preparation). In this way, the layers forming during the concrete placing were modeled. The range of significant correlation was approximately 80 mm in the horizontal direction and 30 mm in the vertical direction (Fig. 8.7). The smaller the λ parameter, the shorter is the correlation range. The dimension of the random field was identical as the finite element mesh. The same random values were assumed in 4 neighboring triangular elements.

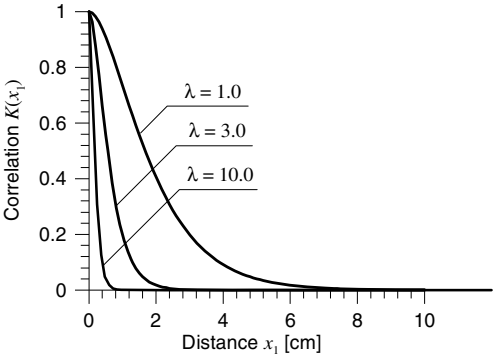

Fig. 8.7 The correlation distances for different coefficients λ [1/m] (Bobiński et al. 2009)

Using the conditional-rejection method, 2000 field realizations of the tensile strength were generated. Next, the generated fields were classified according to two parameters: the mean value of the tensile strength and the gap between the lowest and the highest value of the tensile strength. The joint probability distribution (so-called "ant hill") is presented in Fig. 8.8. One dot represents one random vector described by its mean value and the difference between its extreme values. The two variable domains were divided in 12 intervals of equal probabilities (see vertical and horizontal lines in Fig. 8.8). Next, according to the Latin hypercube sampling assumptions, 12 random numbers in the range 1-12 were generated (one number appeared only once) using the uniform distribution. The generated numbers formed the following 12 pairs: 1 – 4, 2 – 7, 3 – 3, 4 – 11, 5 – 5, 6 – 8, 7 – 1, 8 – 6, 9 – 2, 10 – 9, 11 – 10 and 12 – 12. According to these pairs, the appropriate areas (subfields) were selected (they are presented as rectangles in Fig. 8.9). From each subfield only one realization was chosen and used as the input data for FEM calculations. In this way, the results of 12 realizations were analyzed. Figure 8.9 shows a stochastic distribution of the tensile strength in one arbitrary concrete beam in the area close to the notch.

FE results of deterministic size effect

Figure 8.10 shows the evolution of the calculated normalized vertical force $PL/tf_t(0.9h)^2$ versus the normalized vertical beam displacement u/h for four different beam heights h: 8 cm, 16 cm, 32 cm and 192 cm with constant values of the tensile strength of f_t=3.6 MPa. The thickness of the specimen was equal to t=4 cm (as in laboratory experiments). A distribution of the non-local softening parameter is shown close to the notch (Fig. 8.11). Moreover, the numerical results of a deterministic size effect compared to the size effect model SEL 2 by Bažant for notched concrete specimens (Bažant and Planas 1998) (Eq. 8.2) are shown (Fig. 8.12).

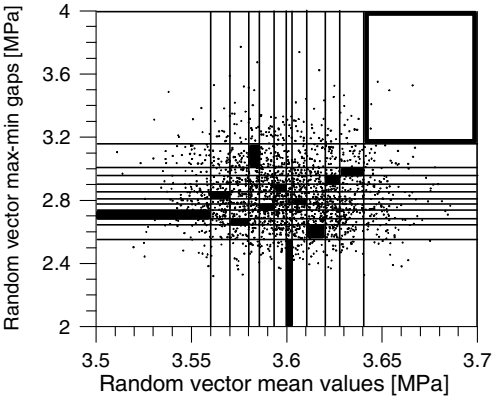

Fig. 8.8 Selection of 12 pairs of random samples using Latin hypercube sampling: 1 – 4, 2 – 7, 3 – 3, 4 – 11, 5 – 5, 6 – 8, 7 – 1, 8 – 6, 9 – 2, 10 – 9, 11 – 10 and 12 – 12 (Bobiński et al. 2009)

The beam strength and beam brittleness obviously increased with increasing beam size. This pronounced deterministic size effect is in agreement with the size effect model by Bažant of Fig. 8.1b (Bažant and Planas 1998). For a very large size beam, a so-called snap-back behaviour occurred (decrease of strength with decreasing deformation). The mean width of a localized zone above the notch was 15.08 mm (h=8 cm), 15.10 mm (h=16 cm), 18.02 mm (h=32 cm) and 18.05 mm (h=192 cm) at u/h=1.000‰, 0.494‰, 0.234‰ and 0.105‰, respectively.

The calculated vertical forces for a small, medium and large beam are in good accordance with the experiments by la Bellego et al. 2003 (Fig. 8.13). The calculated width of the localized zone is similar as in experiments, i.e. about 20 mm (on the basis of acoustic emission, Pijaudier-Cabot et al. 2004).

FE results of statistical size effect

12 selected random samples using Latin hypercube sampling are shown in Fig. 8.8 (λ_{x1}=1 1/m, λ_{x2}=3 1/m, $s_{f_t} = 0.424$). The 12 different evolutions of the vertical normalized force versus the vertical normalized displacement are shown in Fig. 8.14 for 3 different beam heights h: 8 cm (small beam), 32 cm (large beam) and 192 cm (very large beam), respectively. Figure 8.15 demonstrates the calculated width of a localized zone. In turn, 5 arbitrary deformed FE-meshes for a small-size beam are shown in Fig. 8.16. The size effect is shown in Fig. 8.17.

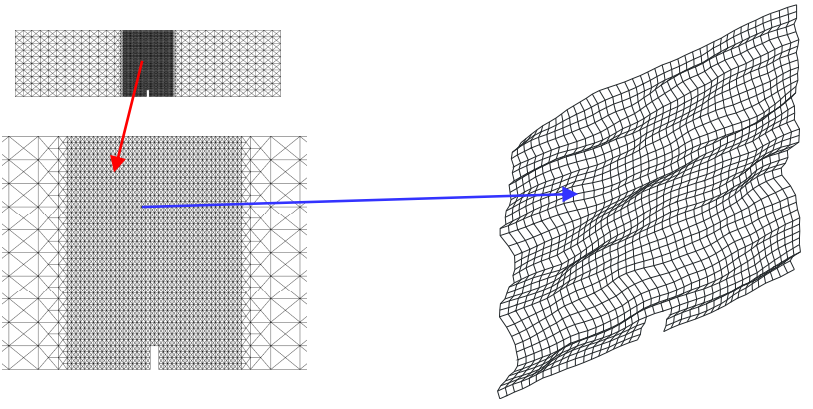

Fig. 8.9 Stochastic distribution of tensile strength f_t close to the notch in small-size beam (strong correlation, small standard deviation) (Bobiński et al. 2009)

The normalized maximum vertical force decreases with decreasing beam height h (Fig. 8.14). For h=8 cm, it changes between 2.92-3.38 kN. The mean stochastic P_{max}=3.08 kN (with the standard deviation of 0.126 kN) is practically the same as the deterministic value P_{max}=3.13 kN (it is smaller by only 2%). If the beam height is h=32 cm, the maximum vertical force varies between 7.73-8.85 and the mean stochastic force P_{max}=8.30 kN (with the standard deviation of 0.334 kN) is smaller by only 0.6% than the deterministic value (P_{max}=8.35 kN). For the beam height of h=192 cm, the maximum vertical force varies between 26.05-28.72 kN and the mean stochastic force P_{max}=27.56 kN is again smaller by only 0.6% than the deterministic value of P_{max}=27.72 kN (the standard deviation equals 0.692 kN).

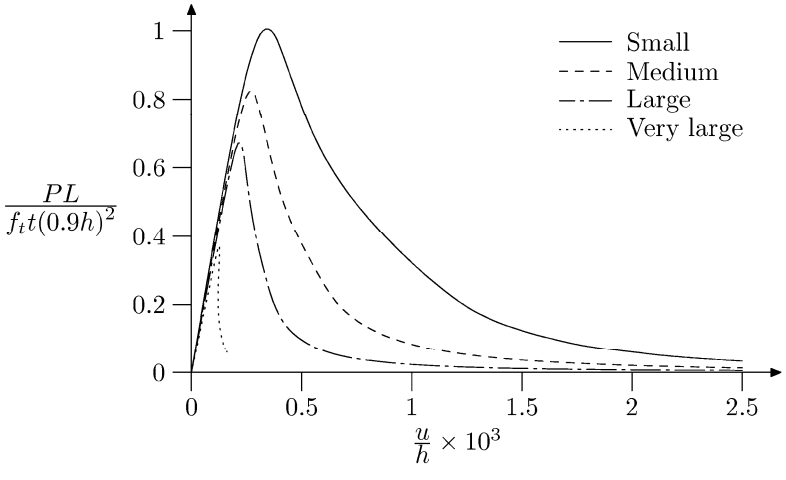

Fig. 8.10 Normalized force-displacement curves with constant values of tensile strength for 4 notched beams under three-point bending (Bobiński et al. 2009)

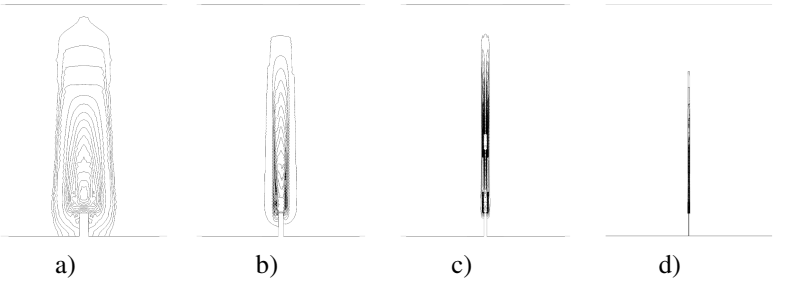

Fig. 8.11 Calculated contours of non-local softening parameter $\overline{\kappa}$ above the notch for three-point bending of small (a), medium (b) large (c) and very large (d) notched concrete beam with constant values of tensile strength (Bobiński et al. 2009)

The stochastic size effect in notched concrete beams is very small; the difference between the deterministic material strength and mean statistical strength is practically negligible.

The load-displacement curves for a very large beam are not smooth in softening regime when the tensile strength is distributed stochastically. The scatter of the maximum vertical force around its mean value is similar for all beam sizes (Fig. 8.17). The deformation field above the notch is strongly non-symmetric (Fig. 8.16). The mean width of the localized zone above the notch is slightly higher than the deterministic value, namely: w=16.56 mm (h=8 cm), w=18.88 mm (h=32 cm) and w=19.67 mm (h=192 cm), Fig. 8.15.

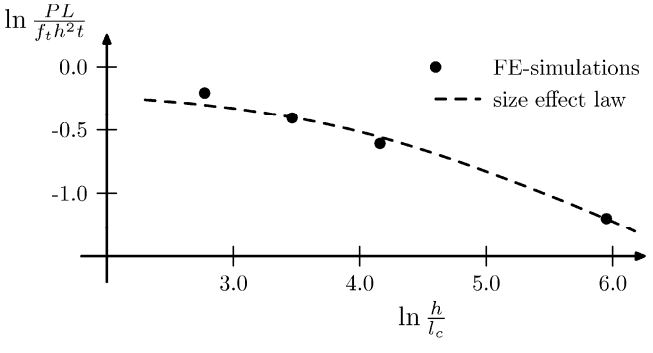

Fig. 8.12 Relationship between calculated normalized concrete strength $\ln\sigma=\ln[PL/(f_t h^2 t)]$ and ratio $\ln(h/l_c)$ compared to size effect law by Bažant of Fig. 8.1b (Bažant and Planas 1998) for constant values of tensile strength (h- beam height, l_c - characteristic length) (Bobiński et al. 2009)

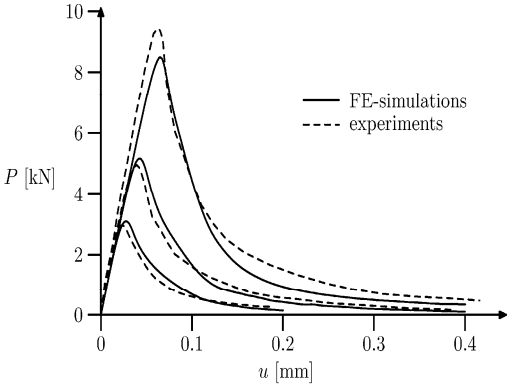

Fig. 8.13 The load-displacement curves from FE-calculations with constant values of tensile strength compared to the experiments by Le Bellego et al. (2003) with 3 notched concrete beams: h=8 cm (lower curves), h=16 cm (medium curves) and h=32 cm (upper curves) (Bobiński et al. 2009)

Our results are close to those given by Vorechovsky (2007). However, in contrast to his results, the difference between stochastic and deterministic values and the scatter of stochastic values in our calculations are similar independently of the beam size. In contrast to simulations by Yang and Xu (2008), which were performed with one notched beam only, the strong tortuousness of crack trajectories was not obtained for a small beam. Beside this fact, the evolution of stochastic load-displacement curves was similar.

Effect of sample number

The calculations were carried out with a small size beam using a direct Monte Carlo method with 30 samples (Fig. 8.18) (λ_{x1}=1 1/m, λ_{x2}=3 1/m, s_{f_t}=0.424 MPa). Almost similar results (mean P_{max}=3.07 kN with s_{f_t}=0.138 MPa) were obtained as in the case of Latin hypercube sampling with 12 samples (mean P_{max}=3.06 kN).

Effect of correlation range

In addition, the calculations were carried out with a small-size beam assuming a very small correlation length of 10 mm (Fig. 8.7) by assuming λ_{x1}=10 1/m, λ_{x2}=10 1/m and $s_{f_t} = 0.424$ MPa in Eq. 8.3. The results (Figs. 8.19 and 8.20) show that the mean stochastic vertical force, P_{max}=3.08 kN, and mean width of the localized zone, w=16.56 mm, are similar as the results with λ_{x1}=1 1/m and λ_{x2}=3 1/m. However, the scatter of forces is significantly smaller.

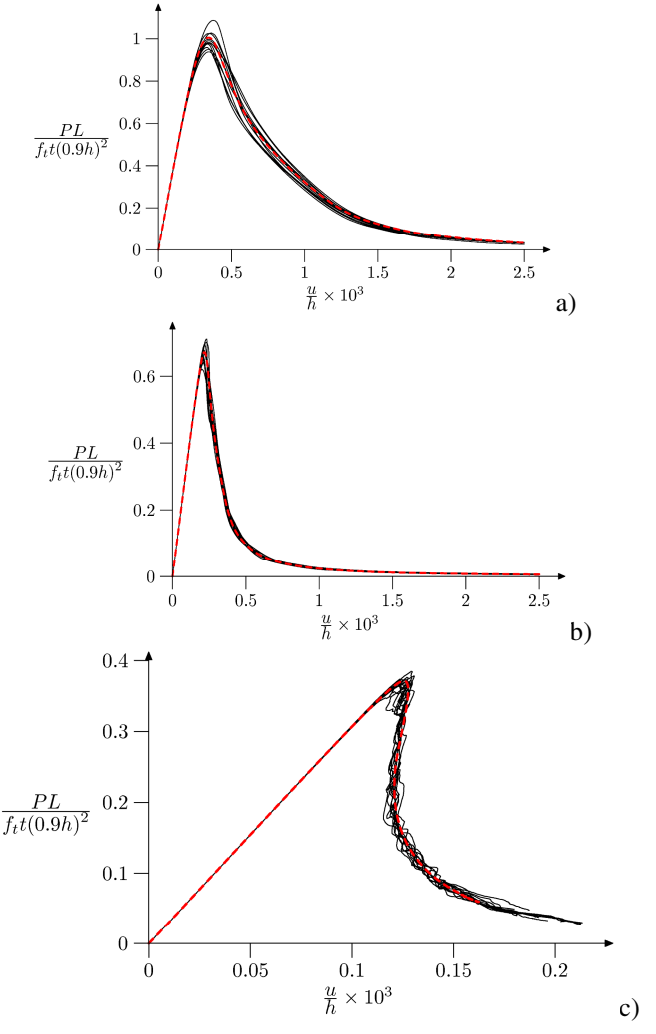

Fig. 8.14 Normalized force-displacement curves in the case of deterministic (red dashed lines) and random calculation (solid lines) for 3 notched beams under three-point bending: a) small-size beam (h=8 cm), b) large-size beam (h=32 cm), c) very large-size beam (h=192 cm) (λ_{x1}=1 1/m, λ_{x2}=3 1/m, s_{fi}=0.424 MPa) (Bobiński et al. 2009)

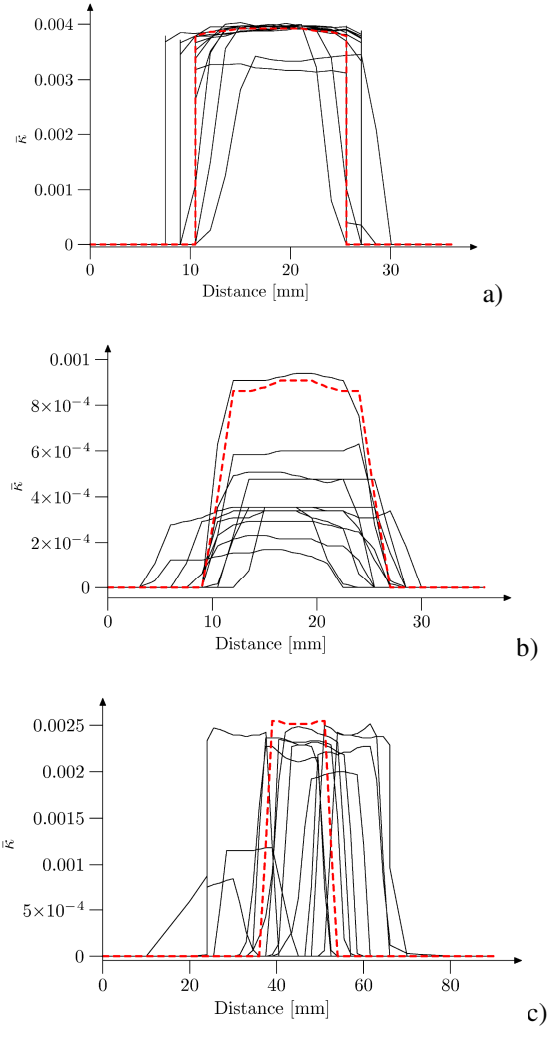

Fig. 8.15 Distribution of non-local softening parameter above the notch in the case of deterministic (red dashed lines) and random calculation (solid lines) for 3 notched beams under three-point bending: a) small-size beam (h=8 cm), b) large-size beam (h=32 cm), c) very large-size beam (h=192 cm) (λ_{x1}=1 1/m, λ_{x2}=3 1/m, s_{ft}=0.424 MPa) (Bobiński et al. 2009)

8.2 Unnotched Beams

Very similar deterministic and stochastic calculations were carried out with concrete beams of Chapter 8.1 without notch using the similar input and material data (Syroka et al. 2011). The two-dimensional FE-analysis of free-supported

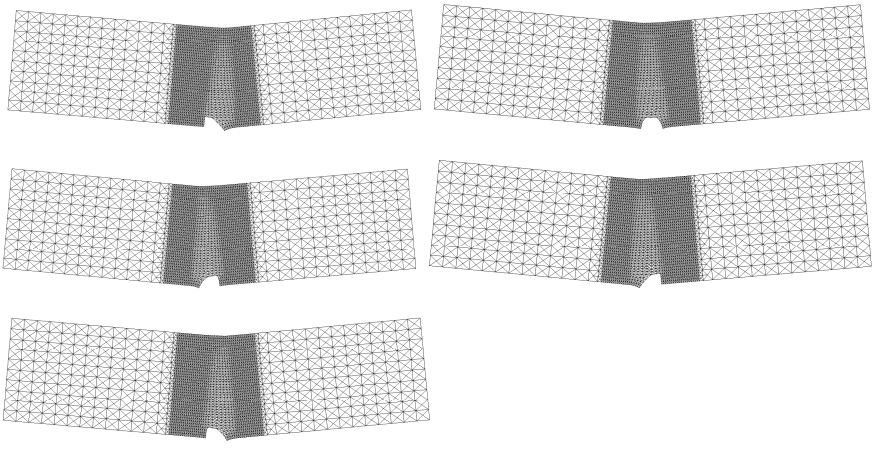

Fig. 8.16 Five arbitrary deformed FE meshes for a small-size beam (h=8 cm, u/h=0.25%) with random distribution of tensile strength (λ_{x1}=1 1/m, λ_{x2}=3 1/m, s_{ft}=0.424 MPa) (Bobiński et al. 2009)

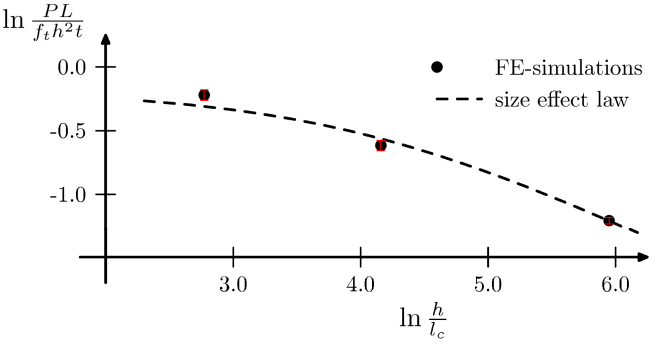

Fig. 8.17 Relationship between calculated normalized concrete strength ln σ=ln [$PL/(f_t h^2 t)$] and ratio ln (h/l_c) compared to the size effect law by Bažant (Bažant and Planas 1998) for stochastic values of tensile strength (Bobiński et al. 2009)

unnotched beams was mainly performed with 4 different beam sizes of a similar geometry $D \times L_t$: 8×32 cm^2 (called small-size beam), 16×64 cm^2 (called medium-size beam), 32×128 cm^2 (called large-size beam), 192×768 cm^2 (called very large-size beam) (D – beam height, L_t – beam length), Fig. 8.21. The span length L was equal to 3D for all beams. The depth of the specimens was t=4 cm. The size $D \times L_t \times t$ of the first 3 beams was similar as in the corresponding experiments carried out by Le Bellego et al. (2003) and Skarżyński et al. (2009). The quadrilateral elements divided into triangular elements were used to avoid

volumetric locking. Totally, 13'820 (small-size beam), 39'900 (medium-size beam), 104'780 (large-size beam) and 521'276 (very large-size beam) triangular elements were used, respectively The computation time varied between 3 hours (small-size beam) and 3 days (very large beam) using PC 3.2 MHz.

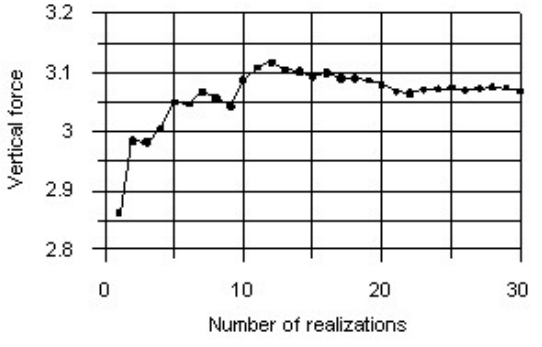

a)

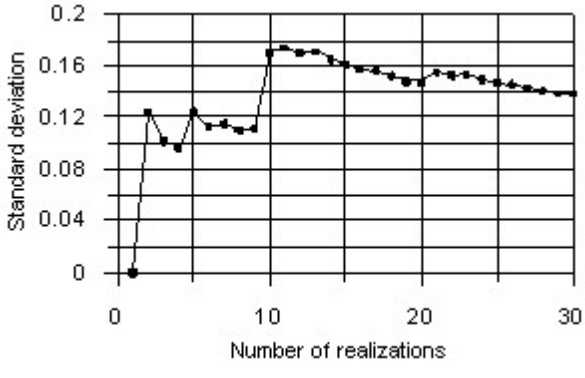

b)

Fig. 8.18 Small size beam with random distribution of tensile strength (h=8 cm) using a direct Monte Carlo method with 30 samples: maximum vertical force with expected values (a) and standard deviation (b) (λ_{x1}=1 1/m, λ_{x2}=3 1/m, s_{ft}=0.424 MPa) (Bobiński et al. 2009)

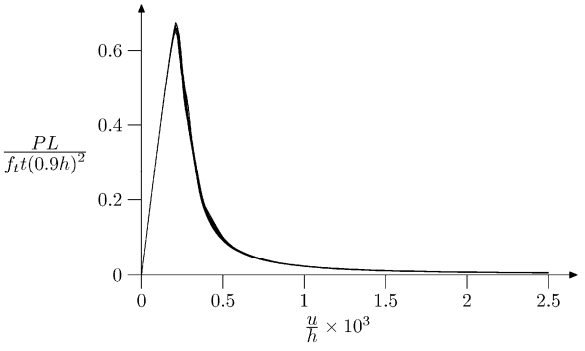

Fig. 8.19 Normalized force–displacement curves with and random distribution of tensile strength for notched small beam under three-point bending (h=8 cm) for smaller correlation length (λ_{x1}=10 1/m, λ_{x2}=10 1/m, $s_{f_t} = 0.424$ MPa) (Bobiński et al. 2009)

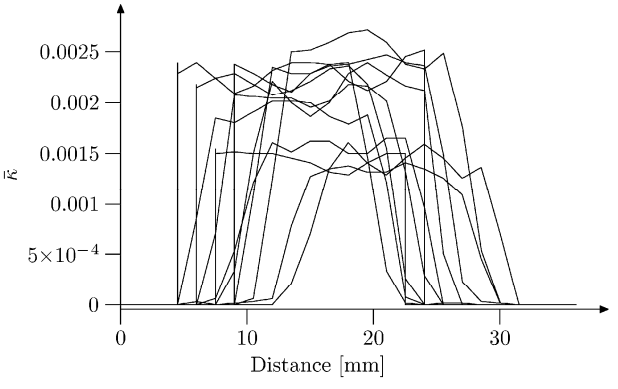

Fig. 8.20 Distribution of non-local softening parameter random distribution of tensile strength for notched small beam under three-point bending (h=8 cm) for small correlation length (λ_{x1}=10 1/m, λ_{x2}=10 1/m, $s_{f_t} = 0.424$ MPa) (Bobiński et al. 2009)

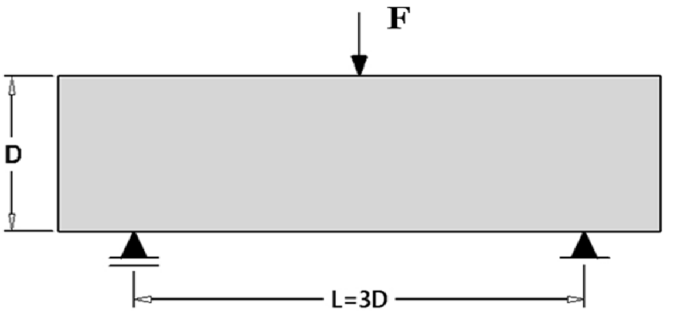

Fig. 8.21 Geometry of free-supported unnotched concrete beams subjected to three-point bending (F – vertical force) (Syroka et al. 2011)

All specimens had again the constant uniformly distributed tensile strength f_t=3.6 MPa. In order to properly capture strain localization in concrete, the mesh was very fine in the mid-part of the beam (Fig. 8.21) (where the element size was not greater than $3\times l_c$). The width of this region s of Fig. 8.22 was determined with preliminary calculations: s=12 cm (D=8 cm), s=18 cm (D=16 cm), s=24 cm (D=32 cm) and s=192 cm (D=192 cm). A quasi-static deformation of a small and medium beam was imposed through a constant vertical displacement increment Δu prescribed at the upper mid-point of the beam top.

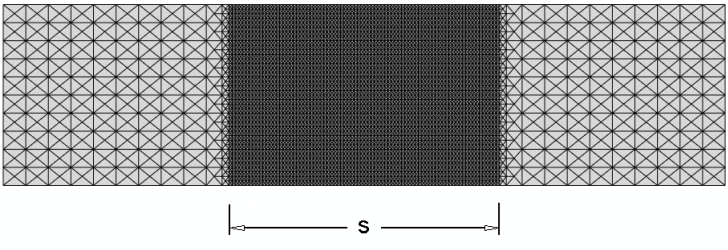

Fig. 8.22 Assumed FE mesh in small-size beam (s – width of region with finer mesh) (Syroka et al. 2011)

Correlated random fields describing a fluctuation of the tensile strength were used to capture a stochastic size effect. The distribution of this single random variable f_t took the form of a truncated Gaussian function with the mean concrete tensile strength of 3.6 MPa (as in calculations with notched beams, Fig. 8.6). The concrete tensile strength values again changed between 1.6 MPa and 5.6 MPa ($f_t = 3.6 \pm 2.0$ MPa). The homogeneous correlation function by Eq. 8.4 was adopted (Bielewicz and Górski 2002). We took again into account a stronger correlation of the tensile strength f_t in a horizontal direction λ_{x1}=1.0 1/m and a

weaker correlation in a vertical directions λ_{x2}=3.0 1/m in Eq. 8.4 (due to the way of the specimen preparation by means of layer-by-layer from the same concrete block). The dimension of the random field was identical as the finite element mesh. The same random values were assumed in four neighbouring triangular elements. To generate the random fields, the conditional-rejection method was again used. The selection was performed by the Latin sampling method (Fig. 8.23). The generated numbers formed the following 12 pairs: 1 – 4, 2 – 7, 3 – 3, 4 – 11, 5 – 5, 6 – 8, 7 – 1, 8 – 6, 9 – 2, 10 – 9, 11 – 10 and 12 – 12 (Fig. 8.23). Figure 8.24 shows the distribution of the concrete tensile strength in a small-size (Fig. 8.24a) and very large-size concrete beam (Fig. 8.24b).

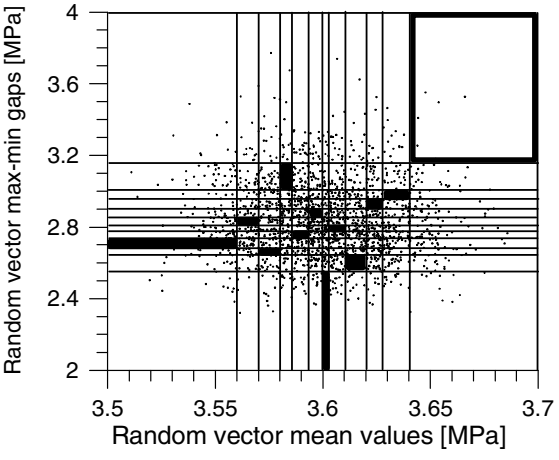

Fig. 8.23 Selection of 12 pairs of random samples using Latin hypercube sampling: 1 – 4, 2 – 7, 3 – 3, 4 – 11, 5 – 5, 6 – 8, 7 – 1, 8 – 6, 9 – 2, 10 – 9, 11 – 10 and 12 – 12 (Syroka et al. 2011)

Deterministic size effect

The evolution of the normalized vertical force $1.5FL/(f_tD^2t)$ versus the normalized deflection u/D for four different beam sizes with the constant values of the tensile strength f_t is shown in Fig. 8.25. The distribution of non-local softening parameter $\bar{\kappa}$ in the mid-region of beams is demonstrated in Fig. 8.26. In Fig. 8.27, our FE results were confronted with FE results for similar notched beams of Chapter 8.1 (Bobiński et al. 2009).

The maximum deterministic vertical forces were: F_{max}=3.83 kN (D=8 cm), F_{max}=6.75 kN (D=16 cm), F_{max}=12.57 kN (D=32 cm) and F_{max}=66.18 kN (D=192 cm), respectively. The strength and ductility strongly increased with decreasing beam height. The normalized nominal (flexural) strength $\sigma_N/f_t=1.5F_{max}L/(D^2tf_t)$ varied between 1.1 (D=192 cm) and 1.5 (D=8 cm). For the large and very large-size beam, the snap-back behaviour occurred. (the strength's decrease with decreasing deformation). It was in particular very strong for the very large-size

beam. Note that the snap-back behaviour happened in notched very large concrete beams only (Bobiński et al. 2009).

The width of a localized zone for all beam sizes was about w=1.5 cm (at the same normalized flexural stress of 1.0, Fig. 8.25). In turn, the height of the localized zone h measured at the peak load increased non-linearly with increasing beam height D, i.e.: 24 mm, 34 mm, 40 mm, and 48 mm for the small (D = 80 mm), medium (D = 160 mm), large (D = 320 mm) and very large beam (D=1920 mm), respectively. The larger the beam, the lower was the ratio of the localized zone height to the beam height h/D: 0.3 (D=80 mm), 0.212 (D=160 mm), 0.125 (D=320 mm) and 0.025 (D=1920 mm).

A pronounced deterministic size effect took place in computations (Fig. 8.27). The deterministic size effect is significantly stronger than in notched concrete beams.

When comparing the numerical results with the size effect model by Bažant (Eq. 8.1), the best fit was achieved with a high parameter r=4 (with f_r^{∞}=3.55 MPa and D_b=112 mm). However, based on the recent results by Bažant et al. (2007a, 2007b), the parameter r (which controls both the curvature and slope of the size effect curve) seems to be close to 1. Therefore, a second deterministic characteristic length l_p was introduced (Bažant et al. 2007a, 2007b) to better describe the size effect law by taking into account a perfect plastic rage for extremely small structure sizes D

$$\sigma_N(D) = f_r^{\infty}\left(1+\frac{rD_b}{l_p+D}\right)^{\frac{1}{r}}. \tag{8.7}$$

This formula represents the full size range transition from the perfectly plastic behaviour (for $D\to 0$, $D\leq l_p$) to the elastic brittle behaviour (for $D\to\infty$, $D>>D_b$) through the quasi-brittle one. The second deterministic characteristic length l_p governs the transition to plasticity for small sizes D. The case $l_p\neq 0$ shows the plastic limit for vanishing size D. This case is asymptotically equivalent to the case of l_p=0 for large D.

The asymptotic prediction for small and large sizes leads to

$$\lim_{D\to 0}\sigma_N(D) = f_r^{\infty}(1+rD_b/l_p) \qquad \text{and} \qquad \lim_{D\to 0}\sigma_N(D) = f_r^{\infty}. \tag{8.8}$$

The parameter l_p equals

$$l_p = \frac{rD_b}{\eta_p - 1} \tag{8.9}$$

with η_p - the ratio between the maximum plastic and elastic strength.

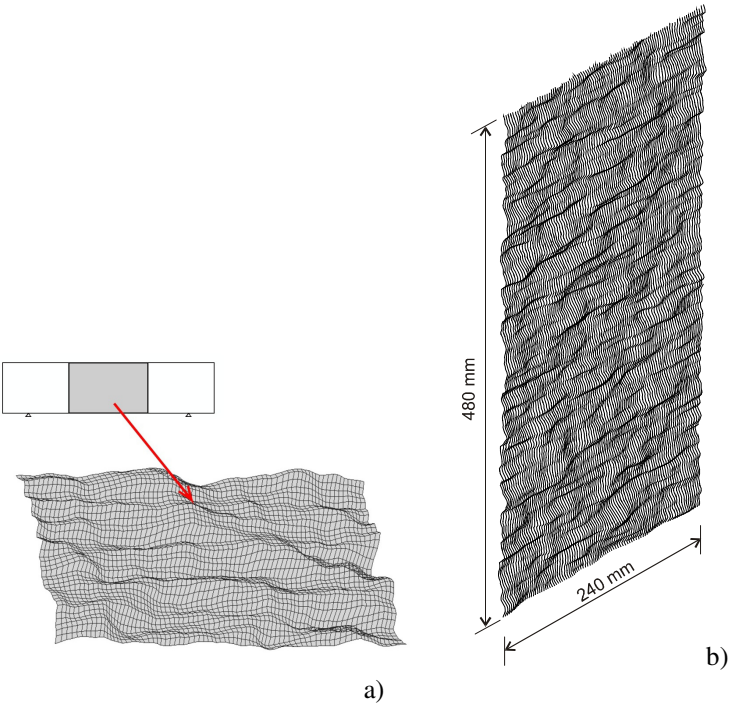

Fig. 8.24 Distribution of concrete tensile strength in small-size concrete beam D=8 cm (region 8×12 cm^2) (a) and in very large-size concrete beam D=192 cm (region 24×48 cm^2) (b) (Syroka et al. 2011)

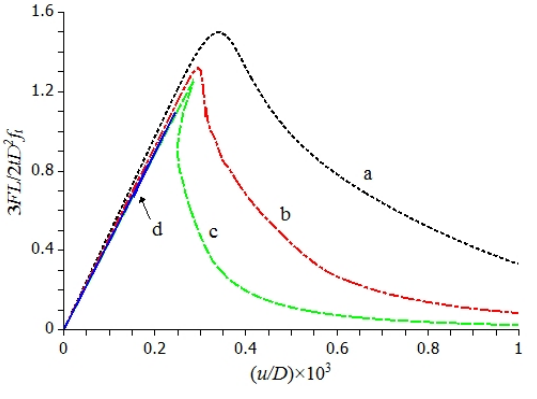

Fig. 8.25 Normalized horizontal normal (flexural) stress-deflection curves $1.5FL/(f_tD^2t)$=f(u/D) under 3-point bending with constant values of tensile strength for 4 different concrete beam heights: small D=8 cm (dashed line 'a'), medium D=16 cm (dotted-dashed line 'b'), large D=32 cm (dotted line 'c'), very large D=192 cm (solid line 'd') (F – vertical force, L – beam length, D – beam height, t- beam thickness, f_t - tensile strength) (Syroka et al. 2011)

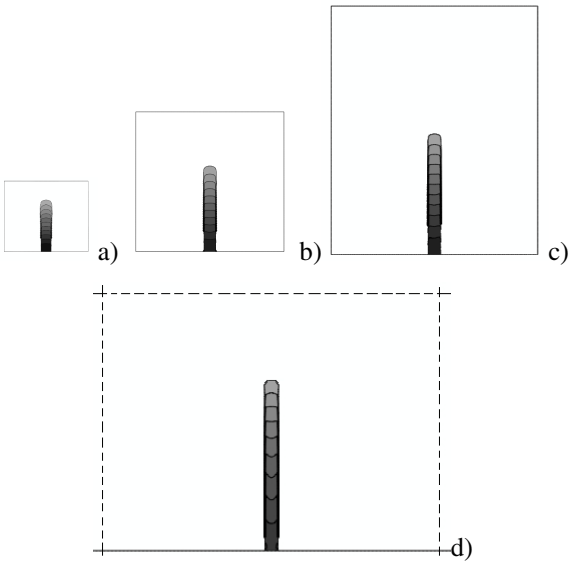

Fig. 8.26 Distributions of non-local softening parameter $\overline{\kappa}$ in concrete beams (mid-region) from deterministic calculations sizes at σ_N=0.45 MPa in: a) small D=8 cm, b) medium D=16 cm, c) large D=32 cm and d) very large-size beam D=192 cm (figure 'd' is not appropriately scaled) (Syroka et al. 2011)

The parameter l_p was determined with additional FE calculations for $D\rightarrow 0$ and $D\rightarrow\infty$. Thus, four additional geometrically similar concrete elements were numerically analyzed by us with D=0.2 cm, D=2 cm, D=4 cm and D=384 cm. On the basis of the nonlinear regression method by Leveneberg-Marquardt, the following parameters were found to fit Eq. 8.7: f_r^{∞}=3.782 MPa, D_b=40 mm, l_p= 13.6 mm, r=1.0. The agreement of our FE results for 8 elements with Eq. 8.7 is almost perfect (Fig. 8.28).

Statistical size effect

The 12 different evolutions of the normalized vertical force $FL/(f_tD^2t)$ versus the normalized vertical deflection u/D from stochastic calculations are shown in Fig. 8.29 (the deterministic curve is also attached).

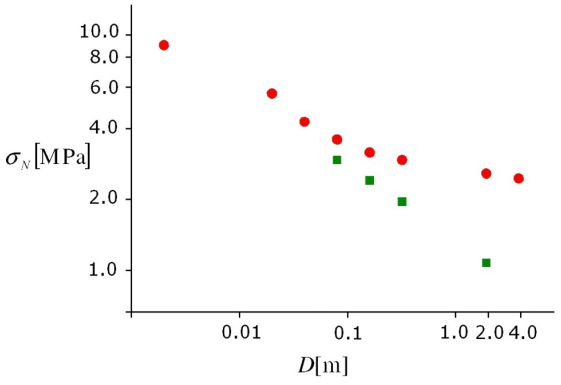

Fig. 8.27 Calculated nominal strength versus beam height from deterministic FE calculations for notched concrete beams (Bobiński et al. 2009, Chapter 8.1) (green diamonds) and unnotched beams (red circles) (Syroka et al. 2011)

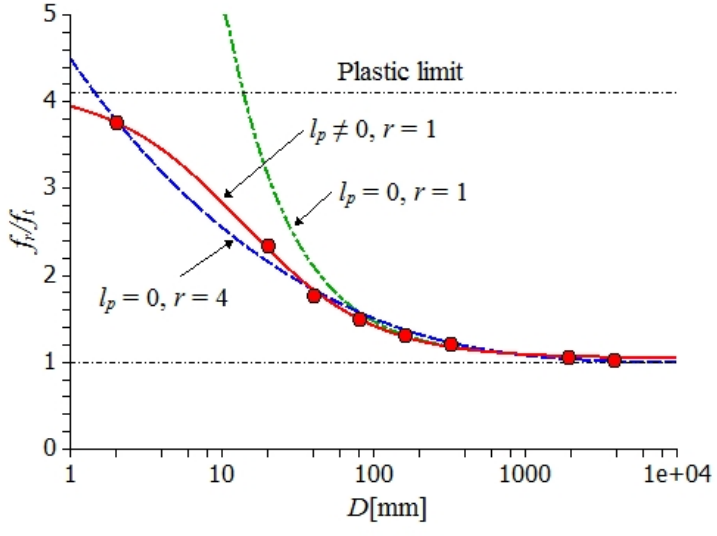

Fig. 8.28 Calculated normalized flexural tensile strength $f_r/f_t=1.5F_{max}L/(f_tD^2t)$ versus beam height D in unnotched concrete beams from deterministic FE calculations (red circles) versus beam height D compared with the deterministic size effect model by Bažant (blue dashed line by Eq. 8.1 with r=1, green dotted line by Eq. 8.1 with r=4 and red solid line by Eq. 8.7 with r=1) (Syroka et al. 2011)

The deterministic normalized vertical force is located in the range of stochastic values for a small and medium-size beam or is the maximum values for a large and very large-size beam. For the height of D=8 cm, the maximum vertical force changes between 3.267-4.08 kN, and the mean value F_{mean}=3.72 kN is by 3%

smaller than the deterministic value F=3.83 kN (the coefficient of variation cov=0.063). If the beam height is D=16 cm, the maximum vertical force varies between 5.61-6.82 kN and the mean stochastic force F_{mean}=6.25 kN (with the coefficient of variation cov=0.057) is smaller by 7% than the deterministic value (F=6.75 kN). For the both beams, the single maximum stochastic vertical force can be higher than the deterministic one. If the beam height is D=32 cm, the maximum vertical force changes between 10.31-12.25 kN, and the mean stochastic F_{mean}=11.07 kN (with the coefficient of variation cov=0.053) is smaller by 12% than the deterministic value of F=12.57 kN. Finally, in the case of the very large-size beam D=192 cm, the maximum vertical force changes between 54.32-59.18 kN and the mean stochastic F_{mean}=57.14 kN (the variation coefficient equals cov=0.027) is smaller by 14% than the deterministic value of F=66.18 kN. Thus, both the mean stochastic nominal strength and coefficient of variation always decrease with increasing size D and the influence of the random distribution of the tensile strength on the nominal strength is stronger for larger structures (Fig. 8.30). In addition, the calculations were carried out with a small-size beam, assuming a correlation length lower than the dimension of a single finite element. A scatter of the vertical force was small (the coefficient of variation strongly depends on the correlation range of correlation).

Figures 8.31-8.33 show some results for a localized zone from stochastic analyses (concerning the propagation way through finite elements with the different tensile strength – Fig. 8.31, zone height – Fig. 8.33 and zone width - Fig. 8.32). The random fields of f_t do not affect the mean width of a localized zone, which is again about 1.5 cm for all beam sizes (Fig. 8.32). A localized zone can be strongly non-symmetric and curved (Figs. 8.31). It occurs at the mean distance of about 2.0 cm (small-size beam) and of about 40 cm (very large-size beam) from the beam-centre (Fig. 8.31). The mean height of localized zones h at peak was closed to the deterministic outcomes.

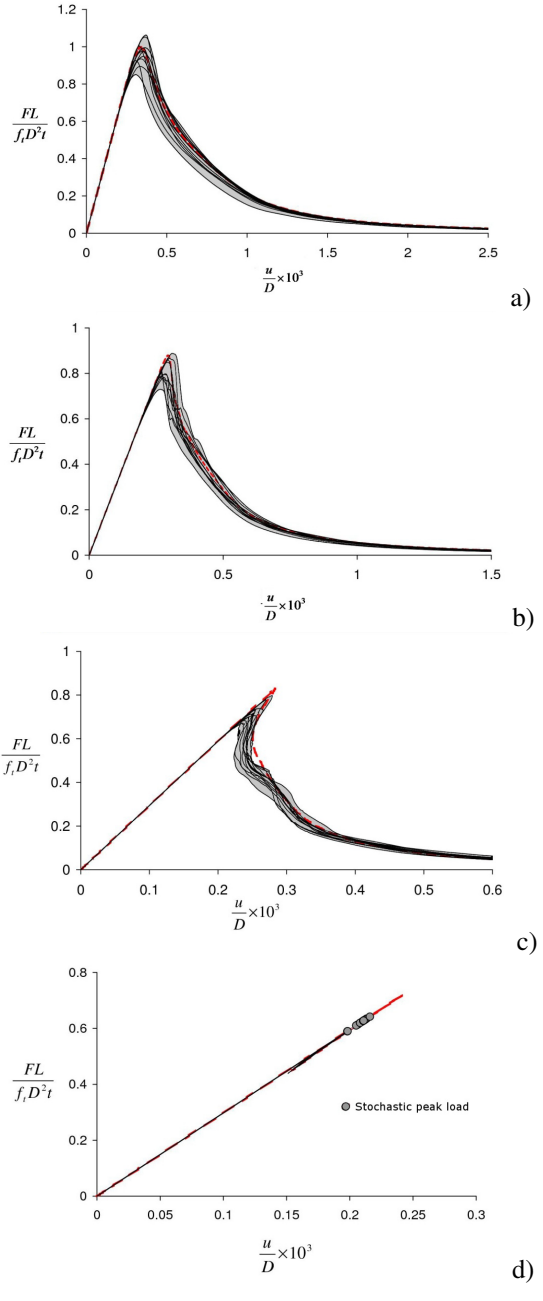

Fig. 8.29 Normalized vertical force-deflection curves with constant (dashed red line) and random (solid lines) value of tensile strength for 4 different beam heights: a) small D=8 cm, b) medium D=16 cm, c) large D=32 cm, d) very large-size beam D=192 cm (Syroka et al. 2011)

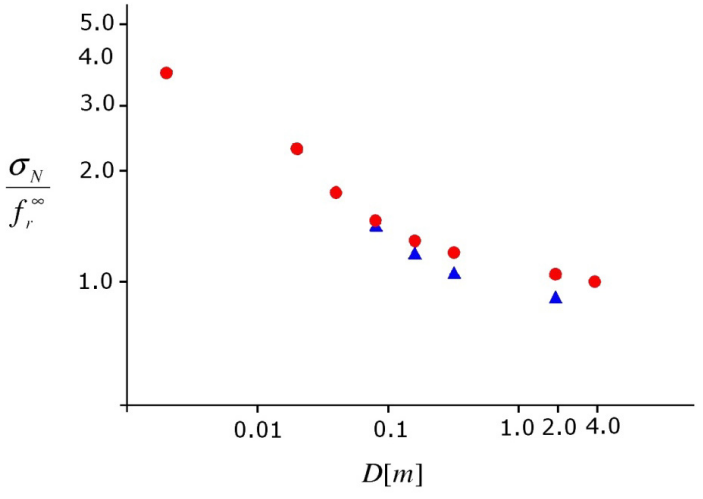

Fig. 8.30 Calculated normalized nominal strength $\sigma_N(D)/f_r^\infty$ versus beam height D from deterministic (circles) and stochastic (triangles) FE calculations for unnotched concrete beams (Syroka et al. 2011)

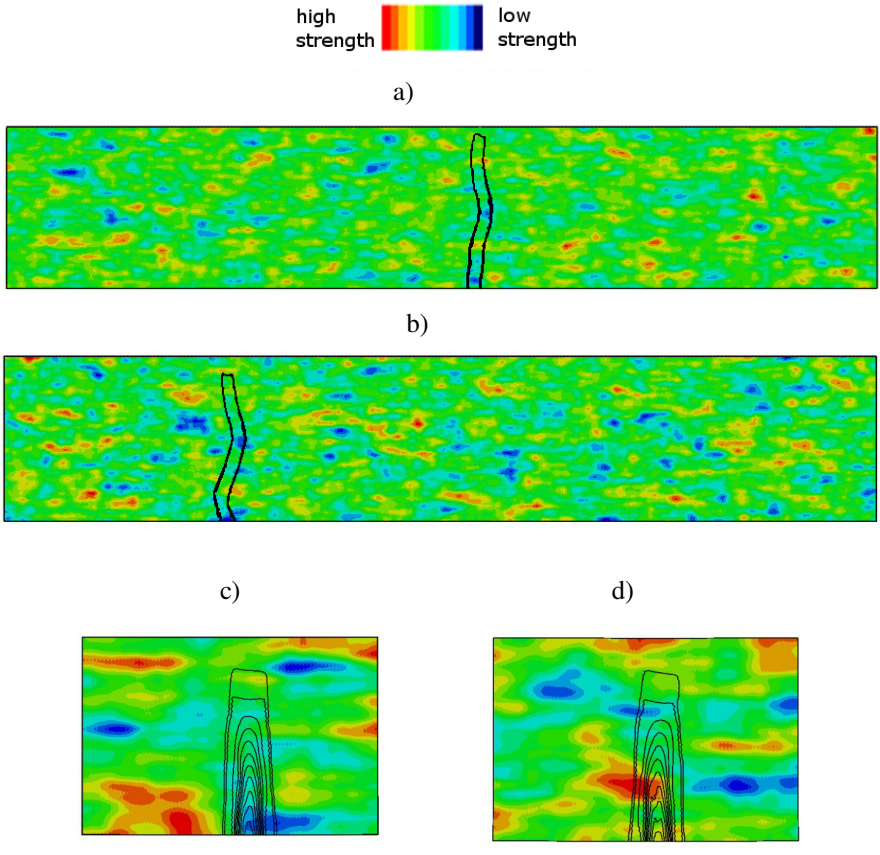

Fig. 8.31 Contours of non-local softening parameter $\overline{\kappa}$ against distribution of tensile strength from stochastic FE calculations in 2 large-size beams D=192 cm and 2 small-size beams D=8 cm (cases 'a' and 'c' correspond to maximum vertical force, cases 'b' and 'd' correspond to minimum vertical force) (tensile strength values are expressed by colour scale) (Syroka et al. 2011)

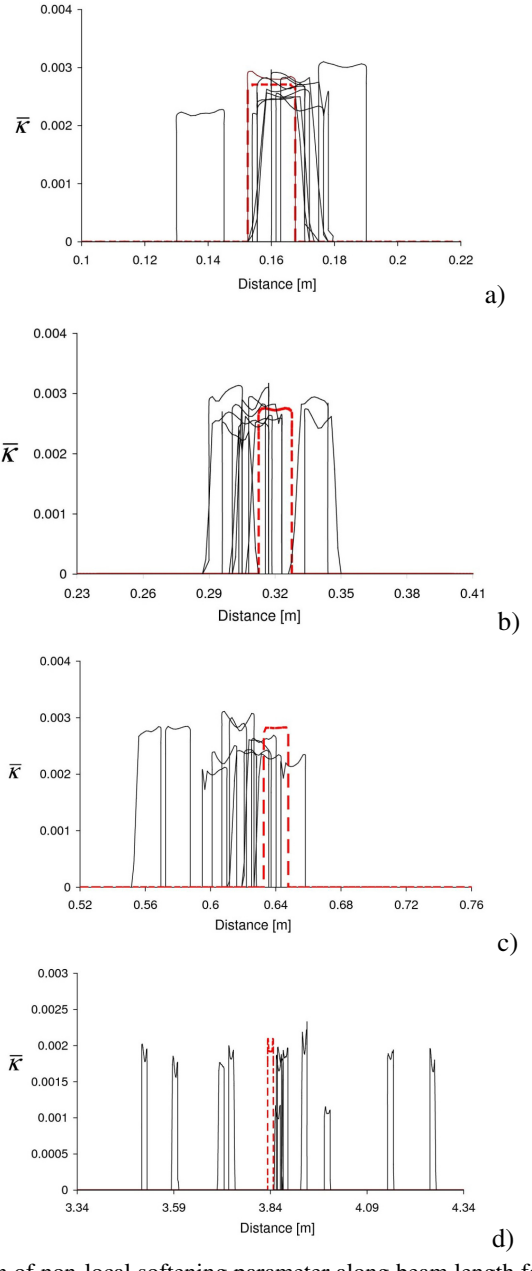

Fig. 8.32 Distribution of non-local softening parameter along beam length for deterministic (dashed lines) and stochastic calculations (solid lines) for 4 beams under three-point bending: a) small D=8 cm, b) medium D=16 cm, c) large D=32 m and d) very large-size beam D=192 cm (Syroka et al. 2011)

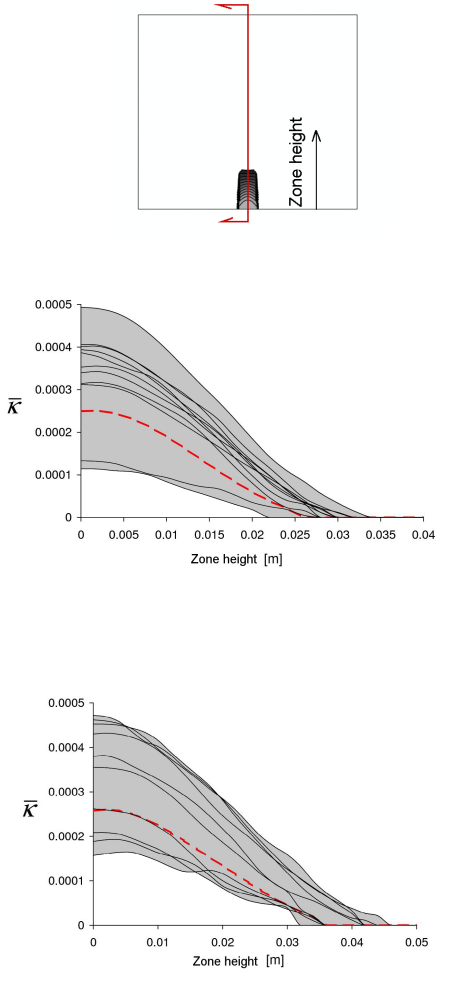

Fig. 8.33 Relationship between non-local softening parameter and localized zone height from deterministic (dashed lines) and stochastic (solid lines) calculations for: a) small D=8 cm, b) medium D=16 cm, c) large D=32 cm and d) very large-size beam D=192 cm (Syroka et al. 2011)

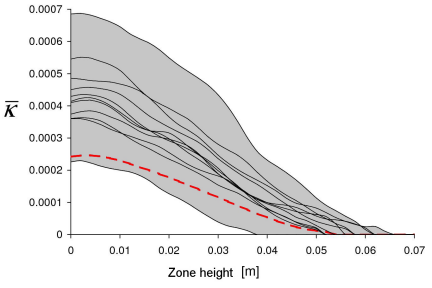

c)

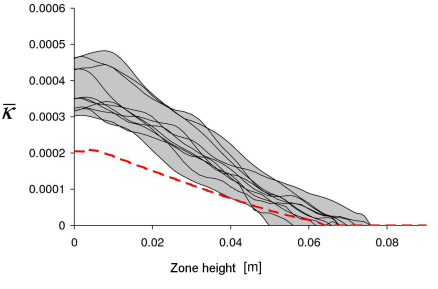

d)

Fig. 8.33 (*continued*)

The maximum vertical force in concrete beams strongly depends on the position of a localized zone. This position is connected with the distribution and magnitude of the tensile strength at the place of a localized zone (within the area $w \times h$) and the magnitude of the horizontal normal stress due to bending σ_{11}. The maximum vertical force increases with increasing ratio $\overline{f}_t(w \times h)/\sigma_{11}$. A localized zone is created, where the mean local tensile strength $\overline{f}_t$ in the localized area $w \times h$ is minimum. In a small-size beam (Figs. 8.31c and 8.31d), the beam mid-region where a localized zone can be created is very limited due to the assumed standard deviation of the tensile strength and correlation range (3 cm in a vertical direction and 8 cm in a horizontal direction). In this limited beam region (with a small number of weak spots, Figs. 8.31c and 8.31d), the tensile strengths are strongly correlated and can be higher or lower than its mean value f_t=3.6 MPa. Therefore, the vertical normal tensile force can be smaller or larger than this in the deterministic study (depending on the spot choice by a localized zone for propagation). With an increase of the beam size, the number of weaker local spots increases with the correlation range assumed (Figs. 8.31a and 8.31b) and the beam mid-region where a localized zone can propagate is significantly larger. In this wide beam region, the tensile strengths are weaker correlated than in a small-size beam. So there exists a very high probability to achieve a smaller vertical force

than in a small beam due to the great number of weak spots with the tensile strength smaller than f_t=3.6 MPa, which can be chosen by a localized zone for propagation (Figs. 8.31a and 8.31b).

An extended universal formula for a coupled deterministic-stochastic size effect law involves a deterministic scaling length D_b and a stochastic scaling length L_o (Bažant et al. 2007a, 2007b)

$$\sigma_N(D) = f_r^{\infty}\left(\left(\frac{L_o}{D+L_o}\right)^{\frac{r\bullet n}{m}} + \frac{rD_b}{D+l_p}\right)^{\frac{1}{r}}, \tag{8.10}$$

where m is the Weibull modulus (responsible for the slope of a large-size asymptote) and n is the number of spatial dimensions (n=2 for 2D problems). Thus, the mean size effect is separately divided into a stochastic part and deterministic. The parameter D_b drives the transition from elastic-brittle to quasi-brittle and L_o drives it from constant property to local Weibull via strength random field. The simplest choice for analyses is usually L_o=D_b. Equation 8.10 satisfies 3 asymptotic conditions: a) for small sizes D→0, it asymptotically reaches the deterministic size effect law (Eq. 8.7), b) for large sizes D→∞, it asymptotically reaches the dominating Weibull size effect with the slope equal to $-n/m$ and c) for m→∞ and L_o→∞, it is equal to the deterministic size effect law. Thus, Eq. 8.10 can be regarded as the asymptotic matching of small-size deterministic and large-size stochastic size effects. With respect to the largest beam, the optimum match for the parameter m is the value of 48 calculated from the coefficient of variation cov (with cov=0.027) - driven by m only

$$cov = \sqrt{\frac{\Gamma\left(1+\frac{2}{m}\right)}{\Gamma^2\left(1+\frac{1}{m}\right)} - 1}\,. \tag{8.11}$$

However, the modulus m in other stochastic FE analyses was equal either to m=24 (Bažant and Novak 2001) or even m=8 (Vorechovsky 2007) with different other parameters (e.g. f_r^{∞}=3.68-3.76 MPa, L_o=D_b=15.53-48.66 mm and r=1.14-1.28, Bažant and Novak 2001). Thus, the stochastic size effect was slightly weaker in our numerical analyses (m=48) being independent of the correlation length. This can be mainly caused by the different loading type (bending versus uniaxial tension), correlation function and sampling type.

Figure 8.34 presents a comparison between our numerical results and size effect law by Bažant (Eqs. 8.7 and 8.10) using the following parameters: L_o= D_b= 30.37 mm, n=2, l_p=0, r =1, m=48 and f_r^{∞}=3.90 MPa with the related asymptotes

assuming the Weibull modulus m=12-48. The stochastic outcomes indicate a further decrease of the nominal strength with increasing element size while the deterministic ones reach their lower limit. Our deterministic-statistical results present also a satisfactory agreement with the size effect law by Bažant by assuming the recommended value of m=24 (L_o=D_b=16.95 mm, l_p=0, r=1 and f_r^{∞}=4.753 MPa). However, the Weibull modulus m=48 solely enables a transition from a pure deterministic to a coupled deterministic-statistical size effect. The value m=12 underestimates the calculated deterministic-statistical flexural tensile strength.

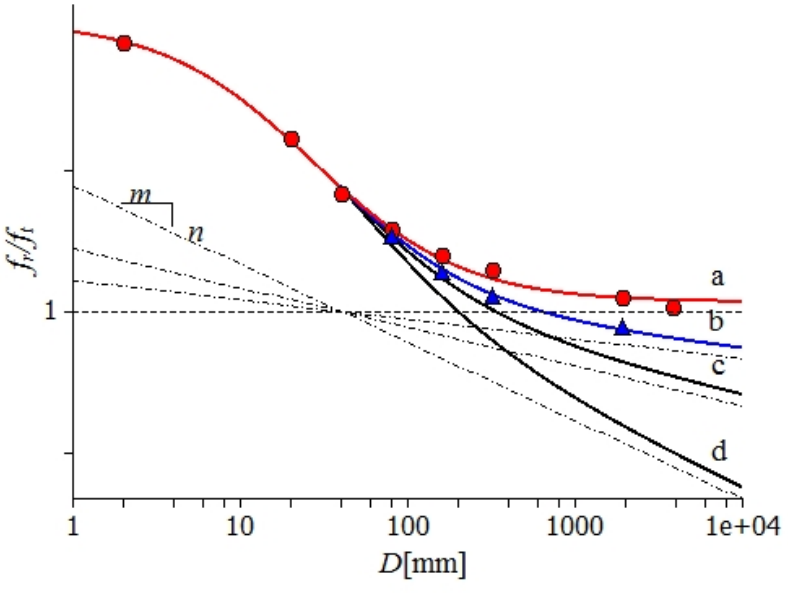

Fig. 8.34 Calculated normalized flexural tensile strength f_r/f_t=1.5$F_{max}L/(f_tD^2t)$ versus beam height D from deterministic (circles) and stochastic (triangles) FE calculations compared with deterministic (line 'a', Eq. 8.7) and deterministic-stochastic size effect law by Bažant (Eq. 8.10) for various Weibull moduli m and constant deterministic parameters (line 'b'- m=48, line 'c'- m=24, line 'd' - m=12) (Syroka et al. 2011)

All size effect results of the normalized nominal (flexural) strength σ_N/f_t=1.5$F_{max}L/(D^2tf_t)$ for unnotched and notched concrete beams (Bobiński et al. 2009) are summarized in Fig. 8.35 as compared to the size effect laws by Bažant (Eqs. 8.2, 8.7 and 8.10): Eq. 8.10 with D_b=40 mm, l_p=13.6 mm, r=1.0, f_r^{∞}= 3.78 MPa, n=2, Eq. 8.7 with m=48, L_o=D_b=40 mm, l_p=13.6 mm, r=1, f_r^{∞}=3.78 MPa, n=2 and Eq. 8.2 with B=1.48 and D_o=0.15 m. For notched structures, a random distribution of the tensile strength has obviously no effect on the nominal strength.

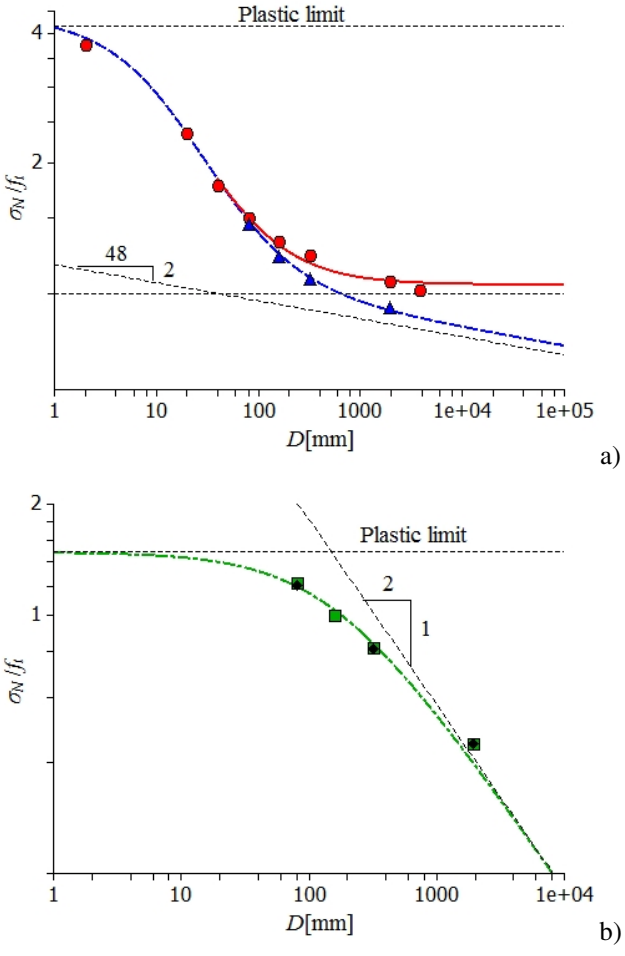

Fig. 8.35 Calculated normalized nominal (flexural) strength σ_N/f_t ($\sigma_N=1.5F_{max}L/(D^2t)$) versus beam height D for: a) unnotched concrete beams from deterministic (red circles) and stochastic (blue triangles); b) for notched concrete beams from deterministic (green squares) and stochastic (green diamonds) FE calculations compared with deterministic size effect law by Bažant (Eq. 8.7) (red solid line), deterministic-stochastic size effect law by Bažant (Eq. 8.10) (blue dashed line) and deterministic size effect law by Bažant (Eq. 8.2) (green dotted-dashed line) (Syroka et al. 2011)

Figures 8.36 and 8.37 compare our FE results on the normalized nominal (flexural) strength with unnotched beams of a coupled deterministic-stochastic size effect with size effect law SEL by Bažant (Eq. 8.10) and MFSL by Carpinteri (Eq. 8.3). In the considered size range of unnotched beams, both size effect laws show almost the same results. In the case of notched beams, there exists, however, a strong discrepancy between the size effect law MFSL (Eq. 8.3 with A_1=2.46 and

A_2=1385.9) and our earlier FE results (Bobiński et al. 2009, Fig. 8.35) for very small (D<0.1 m) and large beams (D>1.0 m) that confirms the conclusions by Bažant and Yavari (2007c) that the size effect law MFSL is not always realistic.

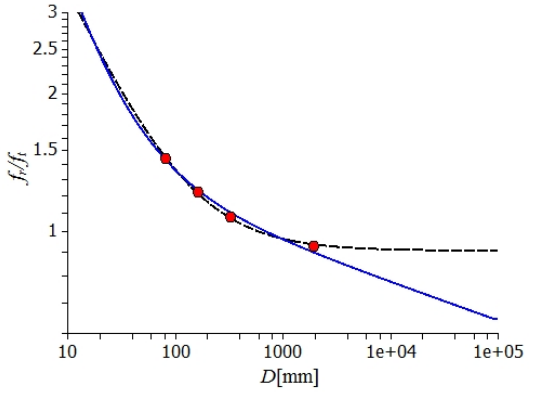

Fig. 8.36 Calculated normalized nominal (flexural) strength f_r/f_t=1.5$F_{max}L/(f_tD^2t)$ versus beam height D from coupled deterministic-stochastic FE calculations (circles) for unnotched beams compared with two size effect laws: SEL by Bažant (Eq. 8.10) – solid line and MFSL by Carpinteri et al. (Eq. 8.3) – dashed line (Syroka et al. 2011)

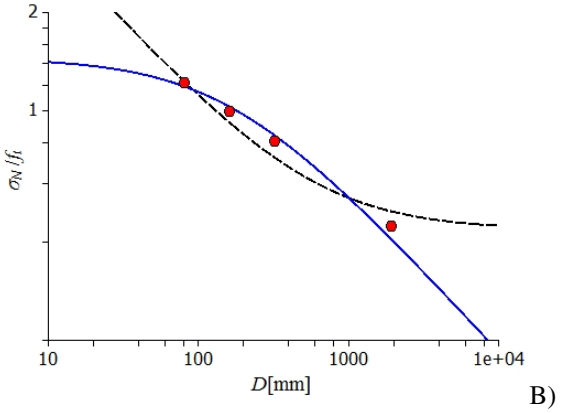

Fig. 8.37 Calculated normalized nominal (flexural) strength σ_N/f_t (σ_N=1.5$F_{max}L/(D^2t)$) versus beam height D from coupled deterministic-stochastic FE calculations (circles) for notched beams (Bobiński et al. 2009) compared with two size effect laws: SEL by Bažant (Eq. 8.2) – solid line and MFSL by Carpinteri et al. (Eq. 8.3) – dashed line (Syroka et al. 2011)

8.3 Elements under Compression

Finally, the effect of an imperfection or notches on a deterministic size effect was investigated during uniaxial compression of a concrete specimen with smooth

boundaries (Skuza and Tejchman 2007). Figure 8.38 presents a hardening-softening curve assumed in compression (Drucker-Prager criterion) (Eqs. 3.27-3.30, 3.93 and 3.97). The Young modulus was E=18000 MPa, Poisson's ratio ν=0.2, compressive strength 32 MPa, non-locality parameter m=2, characteristic length l_c=5 mm, hardening/softening parameter $\kappa_{u2}=3\times10^{-3}$, internal friction angle $\varphi=14^{o}$ and dilatancy angle $\psi=8^{o}$.

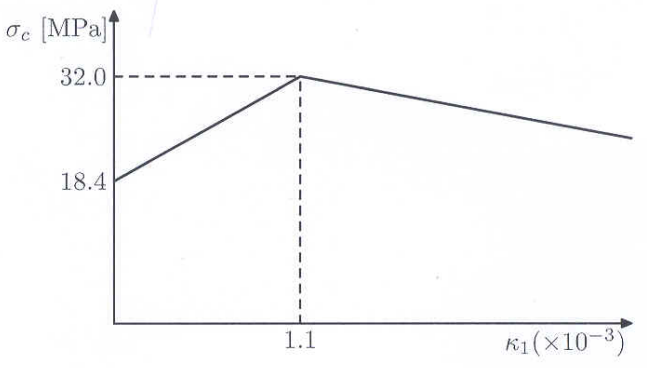

Fig. 8.38 Hardening/softening curve assumed in compression (Skuza and Tejchman 2007)

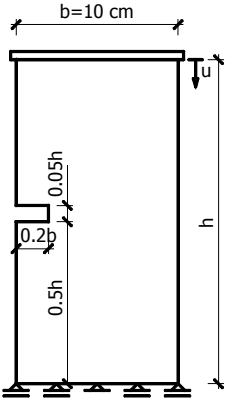

Fig. 8.39 Geometry and boundary conditions of a concrete specimen subjected to uniaxial compression (Skuza and Tejchman 2007)

The FE analyses were performed with 3 different specimens subjected to uniaxial compression: 10×5 cm^2, 10×10 cm^2 and 10×20 cm^2 (Fig. 8.39). The specimens had a weak element or a single notch (mid-point along the left edge). A small deterministic size effect with respect to the strength was obtained in a specimen with a single non-symmetric notch only (Figs. 8.40 and 8.41) due to the fact that damage localization develops faster and is created before the material

strength is attained. This outcome is in agreement with calculations by Cusatis and Bažant (2006) using a 3D lattice model for concrete specimens under uniaxial compression. In concrete specimen under compression, shear zones were obtained during a deformation process (Fig. 8.41). In small specimens, they had a tendency to be reflected from rigid boundaries.

The following conclusions can be drawn from our non-linear FE-investigations of a deterministic and statistical size effect under quasi-static conditions:

- The FE results are in agreement with the size effect law by Bažant (notched and unnotched beams) and by Carpinteri (unnotched beams). However, fractality is not needed to induce a size effect, since the stress redistribution and energy release during strain localization cause a size effect (thus, fractality can contribute to a certain refinement of a size effect but not to its replacement). The size effect model by Bažant is universal and has physical foundations and can be introduced into design codes.
- The deterministic size effect (nominal strength decreases with increasing specimen size) is very pronounced in notched and unnotched concrete beams (it is stronger in notched beams). It is caused by occurrence of a straight tensile localized zone with a certain width. The material ductility increases with decreasing specimen size. A pronounced snap-back behaviour occurs for very large-size notched beams ($h/l_c \approx 400$) and for large and very large-size unnotched beams ($h/l_c \approx 8$). The width of the localized zone is similar for all beam sizes.
- The solution of random non-linear problems on the basis of several samples is possible. The statistical size effect is strong in unnotched concrete beams and negligible in notched concrete beams (due to the same position of the localized zone). The larger the beam, the stronger is the influence of a stochastic distribution on the nominal strength due to the presence of a larger number of local weak spots (i.e. the mean stochastic bearing capacity is always smaller than the deterministic one). The stochastic bearing capacity is larger in some realizations with small and medium-large beams than the deterministic value. The randomness of the tensile strength does not change the mean width of the localized zone. The localized zone can be curved and non-symmetric. This position of the localized zone is connected with the distribution and magnitude of the tensile strength in a localized zone at peak and the magnitude of the horizontal normal stress due to bending.
- The calculated stochastic effect is slightly weaker than in works by Bažant, Novak and Vorechovsky (2006, 2007). This can be mainly caused by the loading type, correlation length, correlation function and sampling type assumed in stochastic calculations. The results obtained with the help of Latin hypercube sampling are strongly influenced by the definition of the beam zone where the tensile strength distribution is statistically described. Our FE results match well the combined deterministic-statistical size effect law by Bažant with the Weibull modulus m=24-48. In turn, a prediction of the combined deterministic-statistical size effect based on deterministic results only is possible with the modulus m=48.

• The deterministic size effect can be observed on specimens under uniaxial compression in presence of non-symmetric notches only. In turn, an increase of ductility with decreasing specimen can be observed in all specimens independently of the imperfection type.

a)

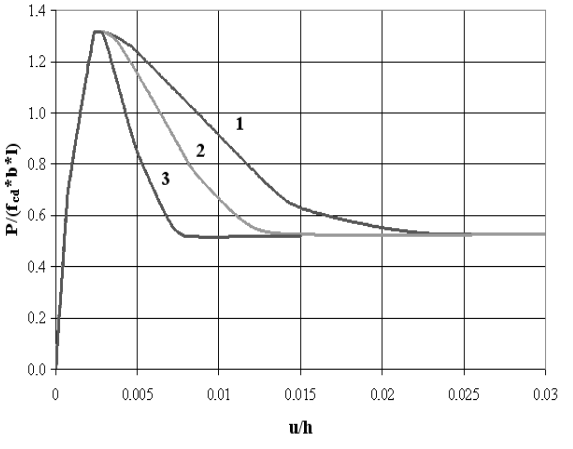

b)

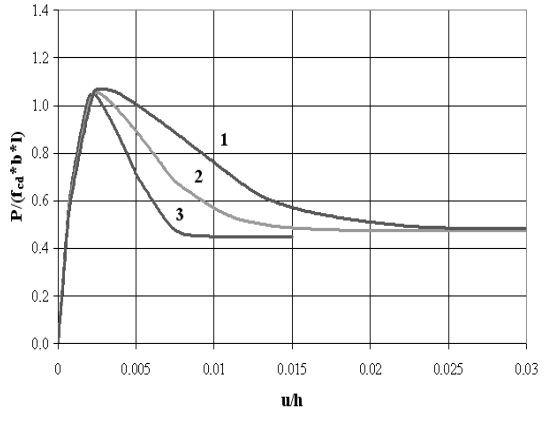

Fig. 8.40 Normalized load-displacement diagrams during uniaxial compression (a) specimen with one weak element, b) specimen with one notch, 1) small-size specimen, 2) medium-size specimen. 3) large-size specimen) (Skuza and Tejchman 2007)

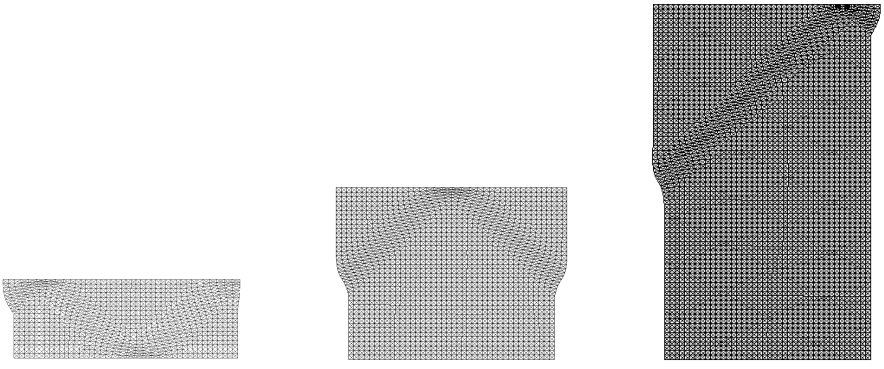

A)

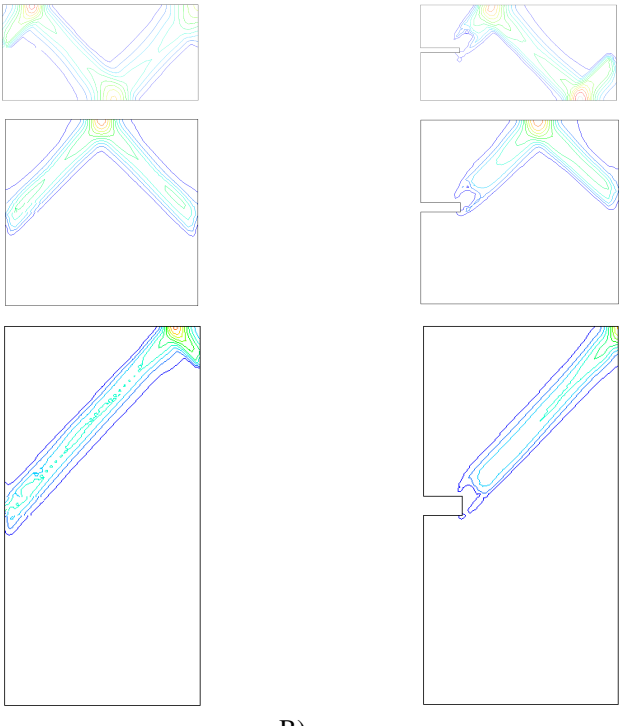

B)

Fig. 8.41 Deformed meshes and contours of non-local softening parameter during uniaxial compression at residual state for small-size, medium-size and large-size concrete specimen: A) unnotched specimens with imperfection, B) specimens with single notch (Skuza and Tejchman 2007)

References

ABAQUS, Theory Manual, Version 5.8, Hibbit. Karlsson & Sorensen Inc. (1998)

Bažant, Z.P.: Size effect in blunt fracture: concrete, rock, metal. Journal of Engineering Mechanics ASCE 110(4), 518–535 (1984)

Bažant, Z.P., Lin, K.L.: Random creep and shrinkage in structures sampling. Journal of Structural Engineering ASCE 111(5), 1113–1134 (1985)

Bažant, Z.P., Chen, E.P.: Scaling of structural failure. Applied Mechanics Reviews 50(10), 593–627 (1997)

Bažant, Z., Planas, J.: Fracture and size effect in concrete and other quasi-brittle materials. CRC Press LLC (1998)

Bažant, Z., Novak, D.: Proposal for standard test of modulus of rupture of concrete with its size dependence. ACI Materials Journal 98(1), 79–87 (2001)

Bažant, Z.: Probability distribution of energetic-statistical size effect in quasibrittle fracture. Probabilistic Engineering Mechanics 19(4), 307–319 (2004)

Bažant, Z.P., Yavari, A.: Is the cause of size effect on structural strength fractal or energetic-statistical? Engineering Fracture Mechanics 72(1), 1–31 (2005)

Bažant, Z., Vorechovsky, M., Novak, D.: Asymptotic prediction of energetic-statistical size effect from deterministic finite-element solutions. Journal of Engineering Mechanics ASCE 133(2), 153–162 (2007a)

Bažant, Z., Pang, S.-D., Vorechovsky, M., Novak, D.: Energetic-statistical size effect simulated by SFEM with stratified sampling and crack band model. International Journal for Numerical Methods in Engineering 71(11), 1297–1320 (2007b)

Bažant, Z., Yavari, A.: Response to A. Carpinteri, B. Chiaia, P. Cornetti and S. Puzzi's comments on "Is the cause of size effect on structural strength fractal or energetic-statistical". Engineering Fracture Mechanics 74(17), 2897–2910 (2007c)

Bielewicz, E., Górski, J.: Shell with random geometric imperfections. Simulation-based approach. International Journal of Non-linear Mechanics 37(4-5), 777–784 (2002)

Bobiński, J., Tejchman, J., Górski, J.: Notched concrete beams under bending – calculations of size effects within stochastic elasto-plasticity with non-local softening. Archives of Mechanics 61(3-4), 1–25 (2009)

Carmeliet, J., Hens, H.: Probabilistic nonlocal damage model for continua with random field properties. Journal of Engineering Mechanics ASCE 120(10), 2013–2027 (1994)

Carpinteri, A.: Decrease of apparent tensile and bending strength with specimen size: two different explanations based on fracture mechanics. International Journal of Solids and Structures 25(4), 407–429 (1989)

Carpinteri, A., Chiaia, B., Ferro, G.: Multifractal scaling law: an extensive application to nominal strength size effect of concrete structures. In: Mihashi, M., Okamura, H., Bažant, Z.P. (eds.) Size Effect of Concrete Structures, vol. 173, p. 185. E&FN Spon (1994)

Carpinteri, A., Chiaia, B., Ferro, G.: Size effects on nominal tensile strength of concrete structures: multifractality of material ligaments and dimensional transition from order to disorder. Materials and Structures (RILEM) 28(180), 311–317 (1995)

Carpinteri, A., Chiaia, B., Cornetti, P., Puzzi, S.: Comments on "Is the cause of size effect on structural strength fractal or energetic-statistical". Engineering Fracture Mechanics 74(14), 2892–2896 (2007)

Chen, J., Yuan, H., Kalkhof, D.: A nonlocal damage model for elastoplastic materials based on gradient plasticity theory. Report Nr.01-13. Paul Scherrer Institute, pp. 1–130 (2001)

Cusatis, G., Bažant, Z.: Size effect on compression fracture of concrete with or without V-notches: a numerical meso-mechanical study. In: Meschke, G., de Borst, R., Mang, H., Bicanic, N. (eds.) Computational Modelling of Concrete Structures, pp. 71–83. Taylor and Francis Group, London (2006)

Elices, M., Guinea, G.V., Planas, J.: Measurement of the fracture energy using three-point bend tests: Part 3—influence of cutting the P -δ tail. Materials and Structures 25(6), 327–334 (1992)

Florian, A.: An efficient sampling scheme: Updated latin hypercube sampling. Probabilistic Engineering Mechanics 7(2), 123–130 (1992)

Frantziskonis, G.N.: Stochastic modeling of hetereogeneous materials – a process for the analysis and evaluation of alternative formulations. Mechanics of Materials 27(3), 165–175 (1998)

Górski, J.: Non-linear models of structures with random geometric and material imperfections simulation-based approach, Habilitation. Gdansk University of Technology (2006)

Gutierrez, M.A., de Borst, R.: Energy dissipation, internal length scale and localization patterning – a probabilistic approach. In: Idelsohn, S., Onate, E., Dvorkin, E. (eds.) Computational Mechanics, pp. 1–9. CIMNE, Barcelona (1998)

Gutierrez, M.A.: Size sensitivity for the reliability index in stochastic finite element analysis of damage. International Journal of Fracture 137(1-4), 109–120 (2006)

Hordijk, D.A.: Local approach to fatigue of concrete. PhD thesis. Delft University of Technology (1991)

Hughes, T.J.R., Winget, J.: Finite Rotation Effects in Numerical Integration of Rate Constitutive Equations Arising in Large Deformation Analysis. International Journal for Numerical Methods in Engineering 15(12), 1862–1867 (1980)

Huntington, D.E., Lyrintzis, C.S.: Improvements to and limitations of Latin hypercube sampling. Probabilistic Engineering Mechanics 13(4), 245–253 (1998)

Hurtado, J.E., Barbat, A.H.: Monte Carlo techniques in computational stochastic mechanics. Archives of Computational Method in Engineering 5(1), 3–30 (1998)

Knabe, W., Przewłócki, J., Różyński, G.: Spatial averages for linear elements for two-parameter random field. Probabilistic Engineering Mechanics 13(3), 147–167 (1998)

Koide, H., Akita, H., Tomon, M.: Size effect on flexural resistance on different length of concrete beams. In: Mihashi, H., Rokugp, K. (eds.) Fracture Mechanics of Concrete, pp. 2121–2130 (1998)

Le Bellego, C., Dube, J.F., Pijaudier-Cabot, G., Gerard, B.: Calibration of nonlocal damage model from size effect tests. European Journal of Mechanics A/Solids 22(1), 33–46 (2003)

McKay, M.D., Conover, W.J., Beckman, R.J.: A comparison of three methods for selecting values of input variables in the analysis of output from a computer code. Technometrics 21(2), 239–245 (1979)

Pijaudier-Cabot, G., Haidar, K., Loukili, A., Omar, M.: Ageing and durability of concrete structures. In: Darve, F., Vardoulakis, I. (eds.) Degradation and Instabilities in Geomaterials. Springer, Heidelberg (2004)

Skarżynski, L., Syroka, E., Tejchman, J.: Measurements and calculations of the width of the fracture process zones on the surface of notched concrete beams. Strain 47(s1), e319–e322 (2011)

Skuza, M., Tejchman, J.: Modeling of a deterministic size effect in concrete elements. Inżynieria i Budownictwo 11, 601–605 (2007) (in Polish)

Syroka, E., Górski, J., Tejchman, J.: Unnotched concrete beams under bending – calculations of size effects within stochastic elasto-plasticity with non-local softening. Internal Report, University of Gdańsk (2011)

Tejchman, J., Górski, J.: Computations of size effects in granular bodies within micro-polar hypoplasticity during plane strain compression. International Journal of Solids and Structures 45(6), 1546–1569 (2007)

Tejchman, J., Górski, J.: Deterministic and statistical size effect during shearing of granular layer within a micro-polar hypoplasticity. International Journal for Numerical and Analytical Methods in Geomechanics 32(1), 81–107 (2008)

Vanmarcke, E.-H.: Random Fields: Analysis and Synthesis. MIT Press, Cambridge (1983)

van Mier, J., van Vliet, M.: Influence of microstructure of concrete on size/scale effects in tensile fracture. Engineering Fracture Mechanics 70(16), 2281–2306 (2003)

van Vliet, M.R.A.: Size effect in tensile fracture of concrete and rock. PhD thesis. University of Delft (2000)

Vorechovsky, M.: Stochastic fracture mechanics and size effect. PhD Thesis. Brno University of Technology (2004)

Vorechovsky, M.: Interplay of size effects in concrete specimens under tension studied via computational stochastic fracture mechanics. International Journal of Solids and Structures 44(9), 2715–2731 (2007)

Walraven, J., Lehwalter, N.: Size effects in short beams loaded in shear. ACI Structural Journal 91(5), 585–593 (1994)

Walukiewicz, H., Bielewicz, E., Górski, J.: Simulation of nonhomogeneous random fields for structural applications. Computers and Structures 64(1-4), 491–498 (1997)

Weibull, W.: A statistical theory of the strength of materials. Journal of Applied Mechanics 18(9), 293–297 (1951)

Wittmann, F.H., Mihashi, H., Nomura, N.: Size effect on fracture energy of concrete. Engineering Fracture Mechanics 33(1-3), 107–115 (1990)

Yang, Z., Xu, X.F.: A heterogeneous cohesive model for quasi-brittle materials considering spatially varying random fracture properties. Computer Methods in Applied Mechanics and Engineering 197(45-48), 4027–4039 (2008)

Yu, Q.: Size effect and design safety in concrete structures under shear. PhD Thesis. Northwestern University (2007)